AD-A110 428 ENVIRONMENTAL RESEARCH INST OF MICHIGAN ANN ARBOR RA--ETC F/G 9/1
ITERATIVE FOURIER SYNTHESIS TECHNIQUES FOR REFLECTION GRATINGS --ETC(U)
OCT 81 K A WINICK F49620-81-C-0029
UNCLASSIFIED ERIM-153900-1-F AFOSR-TR-82-0016 NL

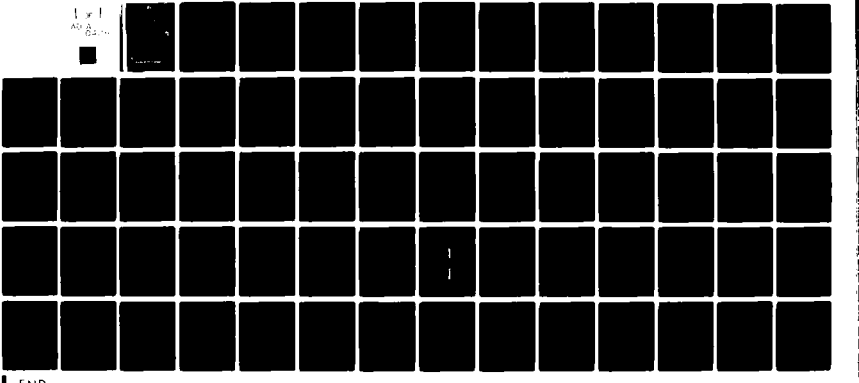

END
DATE FILMED
2-82
DTIC

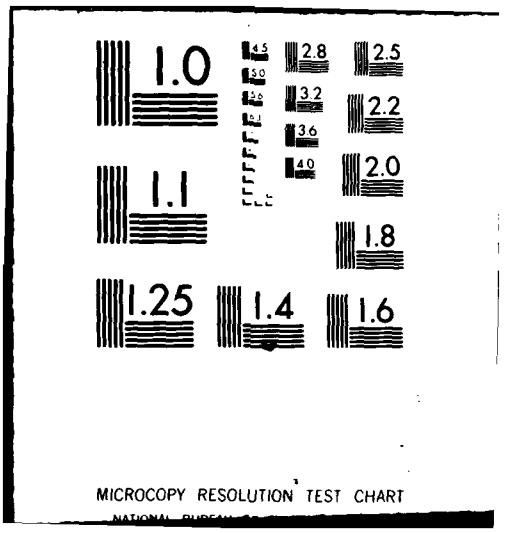
1.0
1.1
1.25
1.4
1.6
1.8
2.0
2.2
2.5
2.8
3.2
3.6
4.0
MICROCOPY RESOLUTION TEST CHART

LEVEL II

Final Scientific Report

ITERATIVE FOURIER SYNTHESIS TECHNIQUES FOR REFLECTION GRATINGS AND CORRUGATED WAVEGUIDE FILTERS

1 February 1981-30 September 1981

K. A. WINICK
Radar and Optics Division

OCTOBER 1981

Directorate of Electronics and Solid State Science
AFOSR/NE, Building 410
Bolling Air Force Base, Washington, DC 20332

ENVIRONMENTAL
RESEARCH INSTITUTE OF MICHIGAN
BOX 8618 • ANN ARBOR • MICHIGAN 48107

UNCLASSIFIED

SECURITY CLASSIFICATION OF THIS PAGE (When Data Entered)

REPORT DOCUMENTATION PAGE	READ INSTRUCTIONS BEFORE COMPLETING FORM
1. REPORT NUMBER **AFOSR-TR- 82 -0016** 2. GOVT ACCESSION NO AD-A110 428	3. RECIPIENT'S CATALOG NUMBER
4. TITLE (and Subtitle) ITERATIVE FOURIER SYNTHESIS TECHNIQUES FOR REFLECTION GRATINGS AND CORRUGATED WAVEGUIDE FILTERS	5. TYPE OF REPORT & PERIOD COVERED Final Scientific Report 1 Feb 1981-30 Sept 1981
	6. PERFORMING ORG. REPORT NUMBER 153900-1-F
7. AUTHOR(s) K. A. Winick	8. CONTRACT OR GRANT NUMBER(s) F49620-81-C-0029
9. PERFORMING ORGANIZATION NAME AND ADDRESS Environmental Research Institue of Michigan Radar and Optics Division, P.O. Box 8618 Ann Arbor, MI 48107	10. PROGRAM ELEMENT, PROJECT, TASK AREA & WORK UNIT NUMBERS 61102F 2305/B1
11. CONTROLLING OFFICE NAME AND ADDRESS Directorate of Electronics and Solid State Science AFOSR/NE, Building 410, Bolling AFB, Washington, DC 20332	12. REPORT DATE October 1981
	13. NUMBER OF PAGES vi + 62
14. MONITORING AGENCY NAME AND ADDRESS (if different from Controlling Office)	15. SECURITY CLASS (of this report) UNCLASSIFIED
	15a. DECLASSIFICATION/DOWNGRADING SCHEDULE N/A

16. DISTRIBUTION STATEMENT (of this Report)

Approved for public release: distribution unlimited.

17. DISTRIBUTION STATEMENT (of the abstract entered in Block 20, if different from Report)

18. SUPPLEMENTARY NOTES

19. KEY WORDS (Continue on reverse side if necessary and identify by block number)
Reflection Grating, Grating Design, Iterative Fourier Synthesis Methods, Integrated Optics, Corrugated Waveguide Filters

20. ABSTRACT (Continue on reverse side if necessary and identify by block number)

This report is divided into three sections. In the first section, the accuracy of coupled mode theory as applied to volume, dielectric reflection gratings which have unslanted fringes and either periodic or aperiodic refractive index profiles is investigated. The accuracy is evaluated by comparing coupled mode theory results with those obtained by Abelès' exact multilayer theory. For the examples considered, coupled mode theory gave accurate results only for gratings having periodic refractive index profiles.

DD FORM 1 JAN 73 1473 EDITION OF 1 NOV 65 IS OBSOLETE

UNCLASSIFIED (continued)

SECURITY CLASSIFICATION OF THIS PAGE (When Data Entered)

20. Abstract (continued)

In Section 2, a method for designing volume, dielectric, reflection gratings having unslanted fringes is developed. The technique is applicable to two types of problems. The first type is one in which the reflectance, R, vs. angle of incidence and wavelength is specified, and the second type is one in which the amplitude reflection and transmission coefficients, r and t, respectively, vs. angle of incidence and wavelength are specified. In both cases, the technique determines (approximately) the corresponding one dimensional refractive index profile, n(z). The synthesis method is illustrated by two examples, and for these examples, the method is seen to be reasonably accurate. In the appendix to Section 2, the reflection grating design approach is extended to multilayer dielectric filters.

In Section 3, a formal mathematical analogy between reflection gratings and corrugated waveguide filters (CWF) is demonstrated. The possibility of designing CWF, using the iterative Fourier transform technique developed in Section 2, is explored. It is emphasized that the mathematics developed for CWF is not rigorous. Consequently, predicted results should be experimentally verified and attempts should be made to develop a rigorous mathematical approach.

PREFACE

This final report was prepared by the Electro-Optics Department, Radar and Optics Division of the Environmental Research Institute of Michigan, The work was sponsored by the Air Force Office of Scientific Research under Contract No. F49620-81-C-0029.

The work covered by this report was performed between 1 February 1981 and 30 September 1981. The contract monitor is Dr. John A. Neff, Directorate of Electronics and Solid State Sciences, AFOSR/NE, Building 410, Bolling Air Force Base, Washington, D.C., 20332. Principal Investigator for this work is K. Winick.

TABLE OF CONTENTS

LIST OF FIGURES

INTRODUCTION

This report is divided into three sections. In the first chapter, the accuracy of coupled mode theory as applied to volume, dielectric, reflection gratings which have unslanted fringes and either periodic or aperiodic refractive index profiles is investigated. The accuracy is evaluated by comparing coupled mode theory results with those obtained by Abele's exact multilayer theory. For the examples considered, coupled mode theory gave accurate results only for gratings having periodic refractive index profiles.

In Section 2, a method for designing volume, dielectric, reflection gratings having unslanted fringes is developed. The technique is applicable to two types of problems. The first type is one in which the reflectance, R, vs. angle of incidence and wavelength is specified, and the second type is one in which the amplitude reflection and transmission coefficients, r and t, respectivly, vs. angle of incidence and wavelength are specified. In both cases, the technique determines (approximately) the corresponding one dimenstional refractive index profile, n(z). The synthesis method is illustrated by two examples, and for these examples, the method is seen to be reasonably accurate. In the appendix to Section 2, the reflection grating design approach is extended to multilayer dielectric filters.

In Section 3, a formal mathematical analogy between reflection gratings and corrugated waveguide filters (CWF) is demonstrated. The possibility of designing CWF, using the iterative Fourier transform technique developed in Section 2, is explored. It is emphasized that the mathematics developed for CWF is not rigorous. Consequently, predicted results should be experimentally verified and attempts should be made to develop a rigorous mathematical approach.

Section 1

ACCURACY OF COUPLED MODE THEORY

In this section, we examine the accuracy of coupled mode theory as applied to volume, dielectric, reflection gratings which have unslanted fringes and either periodic or aperiodic refractive index profiles. The accuracy is determined by comparing coupled mode theory results with those obtained from Abelè's exact multilayer theory. For the examples considered, coupled mode theory gave accurate results only for gratings having periodic refractive index profiles.

1-1. INTRODUCTION

The study of wave propagation through periodic media dates back almost one hundred years, and has had a significant impact in a number of areas including the theory of electron energy bands in crystals, microwave devices, diffraction gratings, and thin film optical devices.[1] Analytic solutions to these wave propagation problems were generally based on Floquet's Theorem.[2] During the 1960's, considerable effort was directed toward finding exact solutions of optical propagation through sinusoidally periodic volume gratings. In particular, C.B. Burckhardt solved the problem of diffraction of a plane wave by a planar, sinusoidal, dielectric transmission grating having unslanted fringes.[3] Unfortunately, the solutions obtained were not in closed form and involved approximate numerical techniques for their evaluation. These numerical techniques were often nontrivial to implement. The numerical difficulties encountered together with the lack of insight gained from these numerical techniques was an impetus for developing a simpler approach.

A natural candidate was coupled mode theory.[4,5] This theory had already been used quite sucessfully to study microwave devices.[6] In many instances, one is interested in a structure into which a small perturbation has been introduced. The modes which propagate in the non-perturbed structure are often easily computed. The perturbation causes some of these modes to interact with one another. Generally the structure is excited in such a manner that a single mode is launched into the structure, and the perturbation causes this mode to excite and exchange energy with other modes as it propagates. In coupled mode theory approximate equations are derived to describe this coupling between modes.

Kogelnik used coupled mode theory to derive closed form expressions for plane wave Bragg diffraction from thick, planar, sinusoidal hologram gratings.[7] The gratings could have arbitrary fringe slant and operate in either the reflection or transmission mode. Kogelnik's results were later extended to periodic gratings having arbitrary shape (i.e. not necessarily sinusoidal).[8]

Unlike Floquet's Theorem, the coupled mode approach does not require that the perturbation be periodic. There has been some interest in producing corrugated waveguide devices for filtering which have nonperiodic corrugations. The characteristics of these structures have been analyzed using coupled mode theory.[9-13] It appears quite difficult to determine bounds on the accuracy of the coupled mode approach. We note, however, that Bragg diffraction from periodic or nonperiodic reflection holograms having zero fringe slant can be solved exactly using a simple multilayer matrix technique developed by Abelè in the 1950's.[14-15] Thus, these reflection grating structures can be used as a check on the accuracy of the coupled mode approach. A reflection hologram of the type discussed above is analogous to corrugated waveguide devices and consequently takes on added importance.[4]

Sakuda,Stoll and Yariv have compared coupled wave theory results and exact results (derived via Floquet's Theorem) for sinusoidally corrugated waveguides.[16-17] Their analysis indicated that the two approaches agree reasonably well. Moharam and Gaylord [18] also ran comparisons for unslanted, sinusoidal, reflection and transmission holograms. For reflection holograms having unslanted fringes, their analysis indicated that the two approaches give results which are in excellent agreement. For slanted fringes they show substantial disagreement, but they have assumed very high refractive index modulations ($\Delta n/n$ as high as 0.29).

In this section we present four examples in which we compare results of coupled wave theory with those of Abelès' exact multilayer theory for reflection gratings having unslanted fringes. The examples show that there is substantial disagreement between the two approaches for gratings having nonperiodic refractive index profiles.

1-2. PROBLEM STATEMENT

Consider a pure dielectric material which has a refractive index variation, $n(z)$, only along the z-axis as shown in Figure 1-1.

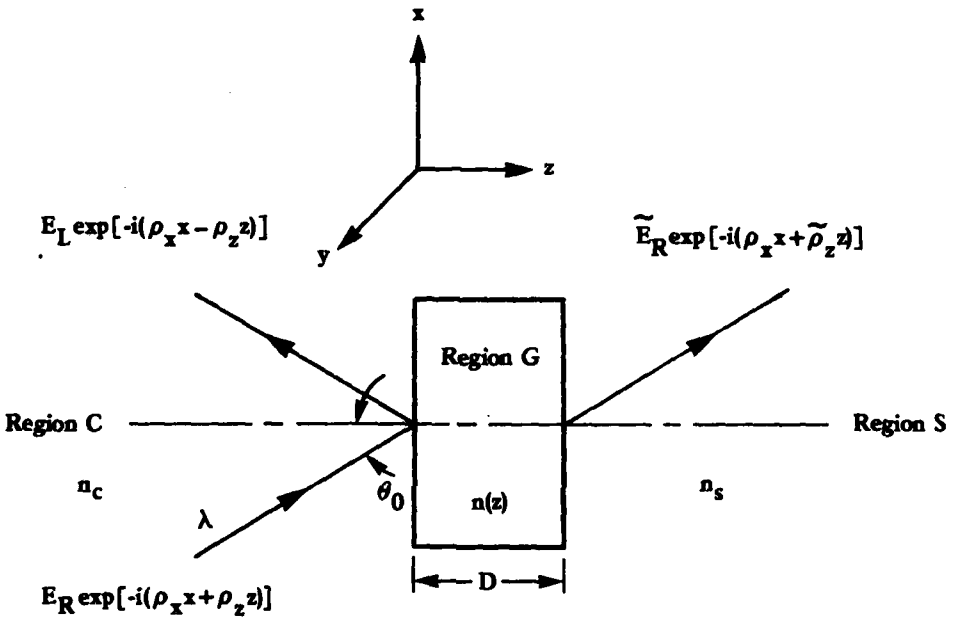

$$\rho_x = \frac{2\pi}{\lambda} n_c \sin\theta_0$$

$$\rho_x^2 + \rho_z^2 = \left(\frac{2\pi}{\lambda} n_c\right)^2$$

$$\rho_x^2 + \tilde{\rho}_z^2 = \left(\frac{2\pi}{\lambda} n_s\right)$$

FIGURE 1-1. DIELECTRIC MATERIAL HAVING A REFRACTIVE INDEX VARIATION IN THE Z DIRECTION. Also shown are incident, reflected and transmitted beams.

The refractive index variation is written as

$$n(z) = n_0 + \Delta n(z)\sin(2\pi f(z)z) \tag{1-1}$$

where

$$\Delta n(z) << n_0 \tag{1-2}$$

The material is assumed to be of infinite extent in both the x and y dimensions. Regions C and S shown in Figure 1-1 have refractive indices $n_C = n(o)$ and $n_S = n(D)$ respectively. An s polarized (electric field along the y axis) plane wave of wavelength λ is incident upon the material. Some of this incident field is reflected, and the remainder is transmitted. The incident electric field amplitude is designated E_R, while the reflected and transmitted electric field amplitudes are designated E_L and $\tilde{E}_R$ respectively. We wish to determine the reflection and transmission coefficients r and t defined by

$$r \triangleq \frac{E_L}{E_R} \tag{1-3a}$$

$$t \triangleq \frac{\tilde{E}_R}{E_R} \tag{1-3b}$$

The general procedure for determining r and t is to solve Maxwell's Equations in the three regions shown in Figure 1-1, and then match the tangential electric field and magnetic field components of these solutions at the boundaries separating regions C and G and regions G and S.

We proceed as follows: The wave equation in all three regions can be written as

$$\nabla^2 E_y(x,z) + \left(\frac{2\pi}{\lambda}\right)^2 n^2(z) E_y(x,z) = 0 \tag{1-4}$$

where E_y is the electric field component along the y axis. Since $\Delta n(z) << n_0$, we can write

$$n^2(z) \simeq n_0^2 + 2n_0\Delta n(z) \sin 2\pi f(z)z \tag{1-5}$$

In region G, Eq. (1-4) has a solution of the form

$$E_y(x,z) = A(z)\exp(-i(\rho_x x + \rho_z z)) + B(z)\exp(-i(\rho_x x - \rho_z z)) \quad (1\text{-}6)$$

where

$$\rho_x \overset{\Delta}{=} \frac{2\pi}{\lambda} n_o \sin\theta \quad (1\text{-}7a)$$

$$\rho_z \overset{\Delta}{=} \frac{2\pi}{\lambda} n_o \cos\theta \quad (1\text{-}7b)$$

Substituting Eqs. (1-5) and (1-6) into Eq. (1-4) yields

$$\begin{aligned}
&A''(z)\exp(-i(\rho_x x + \rho_z z)) - 2i\rho_z A'(z)\exp(-i(\rho_x x + \rho_z z)) \\
&- \rho_z^2 A(z)\exp(-i(\rho_x x + \rho_z z)) - \rho_x^2 A(z)\exp(-i(\rho_x x + \rho_z z)) \\
&+ B''(z)\exp(-i(\rho_x x - \rho_z z)) + 2i\rho_z B'(z)\exp(-i(\rho_x x - \rho_z z)) \\
&- \rho_z^2 B(z)\exp(-i(\rho_x x - \rho_z z)) - \rho_x^2 B(z)\exp(-i(\rho_x x - \rho_z z)) \\
&+ \left(\frac{2\pi}{\lambda} n_o\right)^2 A(z)\exp(-i(\rho_x x + \rho_z z)) + \left(\frac{2\pi}{\lambda} n_o\right)^2 B(z)\exp(-i(\rho_x x - \rho_z z)) \\
&- i\left(\frac{2\pi}{\lambda}\right)^2 n_o \Delta n(z)\, A(z)\exp(-i(\rho_x x + \rho_z z) + i2\pi f(z)z \\
&+ i\left(\frac{2\pi n_o}{\lambda}\right)^2 \Delta n(z)\, A(z)\exp(-i(\rho_x x + \rho_z z) - i2\pi f(z)z \\
&- i\left(\frac{2\pi}{\lambda}\right)^2 n_o \Delta n(z)\, B(z)\exp(-i(\rho_x x - \rho_z z) + i2\pi f(z)z \\
&+ i\left(\frac{2\pi}{\lambda}\right)^2 n_o \Delta n(z)\, B(z)\exp(-i(\rho_x x - \rho_z z) - i2\pi f(z)z = 0
\end{aligned} \quad (1\text{-}8)$$

Using Eqs. (1-7a) and (1-7b), Eq. (1-8) reduces to

$$\begin{aligned}
&A''(z)\exp(-i(\rho_x x + \rho_z z) - 2i\rho_z A'(z)\exp(-i(\rho_x x + \rho_z z)) \\
&+ B''(z)\exp(-i(\rho_x x - \rho_z z)) + 2i\rho_z B'(z)\exp(-i(\rho_x x - \rho_z z))
\end{aligned}$$

$$- i\left(\frac{2\pi}{\lambda}\right)^2 n_o \Delta n(z)\, A(z) \exp(-i(\rho_x x - \rho_z z) + i\Delta\beta(z)z)$$

$$+ i\left(\frac{2\pi}{\lambda}\right)^2 n_o \Delta n(z)\, A(z) \exp(-i(\rho_x x + 3\rho_z z) - i\Delta\beta(z)z)$$

$$- i\left(\frac{2\pi}{\lambda}\right)^2 n_o \Delta n(z)\, B(z) \exp(-i(\rho_x x - 3\rho_z z) + i\Delta\beta(z)z)$$

$$+ i\left(\frac{2\pi}{\lambda}\right)^2 n_o \Delta n(z)\, B(z) \exp(-i(\rho_x x + \rho_z z) - i\Delta\beta(z)z) = 0 \qquad (1\text{-}9)$$

where

$$\Delta\beta(z) \overset{\Delta}{=} 2\pi f(z) - 2\rho_z \qquad (1\text{-}10)$$

It is important to note that no approximations have been made in the derivation leading up to Eq. (1-10).

1-3. COUPLED MODE THEORY

It is common in coupled mode theory to derive from Eq. (1-9) two coupled mode differential equations when $\Delta\beta(z)$ is small. First, it is assumed that only terms in Eq. (1-9) which have approximately the same phase factors will significantly interact with one another. Second, it is assumed that A(z) and B(z) change phase slowly as compared to $\exp(-ip_z z)$. With these assumptions Eq. (1-9) becomes

$$A''(z) - 2i\rho_z A'(z) + i\left(\frac{2\pi}{\lambda}\right)^2 n_o \Delta n(z) \exp(-i\Delta\beta(z)z) B(z) = 0 \qquad (1\text{-}11a)$$

$$B''(z) + 2i\rho_z B'(z) - i\left(\frac{2\pi}{\lambda}\right)^2 n_o \Delta n(z) \exp(i\Delta\beta(z)) A(z) = 0 \qquad (1\text{-}11b)$$

Eqs. (1-11a) and (1-11b) are further simplified by making the assumption that

$$|A''(z)| << |\rho_z A'(z)| \text{ and } |B''(z)| << |\rho_z B'(z)| \qquad (1\text{-}12)$$

With the above approximation, Eqs. (1-11a) and (1-11b) become

$$A'(z) = \frac{1}{2\rho_z}\left(\frac{2\pi}{\lambda}\right)^2 n_0 \Delta n(z) \exp(-i\Delta\beta(z)z) B(z) \qquad (1\text{-}13a)$$

$$B'(z) = \frac{1}{2\rho_z}\left(\frac{2\pi}{\lambda}\right)^2 n_0 \Delta n(z) \exp(i\Delta\beta(z)z) A(z) \qquad (1\text{-}13b)$$

Eqs. (1-13a) and (1-13b) are the first order coupled mode equations which commonly appear in the literature. Since the refractive index is continuous across the boundaries between regions C and G and regions G and S, Maxwell's boundary conditions require

$$A(0) = E_R \qquad (1\text{-}14a)$$

$$B(0) = E_L \qquad (1\text{-}14b)$$

$$A(D) = \tilde{E}_R \qquad (1\text{-}14c)$$

$$B(D) = 0 \qquad (1\text{-}14d)$$

Thus,

$$r = \frac{B(0)}{A(0)} \qquad (1\text{-}14e)$$

$$t = \frac{A(D)}{A(0)} \qquad (1\text{-}14f)$$

1-4. ABELÈS' EXACT MULTILAYER THEORY

In the 1950's Abelès developed a convenient numerical matrix technique for solving Eq. (1-9).[14] First, the structure shown in Figure 1-1 is divided into thin slabs each parallel to the x-y plane. The slabs are chosen to be sufficiently thin so that the refractive index n(z) can be assumed constant within each thin slab. Thus, a solution of the wave equation within the m^{th} thin slab, which is assumed to have a constant refractive index of n_m, is

$$E_{ym}(x,z) = A_m \exp(-i(\rho_{xm}x + \rho_{zm}z)) + B_m \exp(-i(\rho_{xm}x - \rho_{zm}z)) \qquad (1\text{-}15)$$

where

$$\rho_{xm} \triangleq \frac{2\pi}{\lambda} n_m \sin \theta_m \tag{1-16a}$$

$$\rho_{zm} \triangleq \frac{2\pi}{\lambda} n_m \cos \theta_m \tag{1-16b}$$

For m = 0 and m = N+1 Eq. (1-15) is also a solution of the wave equation in the half space regions C and S respectively.

By requiring the tangential components of the electric and magnetic fields to be continuous across the boundaries between the slabs, it is straightforward to show that

$$\begin{bmatrix} A_m \\ B_m \end{bmatrix} = V_m^{-1} V_{m+1} U_{m+1} \begin{bmatrix} A_{m+1} \\ B_{m+1} \end{bmatrix} \tag{1-17}$$

where

$$n_{m+1} \sin \theta_{m+1} = n_m \sin \theta_m \tag{1-18}$$

$$Y_m = \frac{n_m \cos \theta_m}{z_o} \quad (z_o \text{ is the characteristic impedance of free space}) \tag{1-19}$$

$$\phi_m \triangleq \frac{2\pi}{\lambda} n_m d_m \cos \theta_m \quad (d_m \text{ is the thickness of the } m^{th} \text{ thin slab}) \tag{1-20}$$

$$V_m \triangleq \begin{bmatrix} 1 & 1 \\ Y_m & -Y_m \end{bmatrix} \tag{1-21}$$

$$U_m \triangleq \begin{bmatrix} \exp(i\phi_m) & 0 \\ 0 & \exp(-i\phi_m) \end{bmatrix} \tag{1-22}$$

Now with the following definitions

$$M_m \triangleq V_m U_m V_m^{-1} \tag{1-23}$$

$$U_o \triangleq U_{N+1} = \begin{bmatrix} 1 & 0 \\ 0 & 1 \end{bmatrix} \tag{1-24}$$

$$S \triangleq \begin{bmatrix} S_{11} & S_{12} \\ S_{21} & S_{22} \end{bmatrix} \triangleq V_0^{-1} \left(\prod_{m=1}^{N+1} M_m \right) V_{N+1} \tag{1-25}$$

it immediately follows that

$$\begin{bmatrix} A_o \\ B_o \end{bmatrix} = S \begin{bmatrix} A_{N+1} \\ B_{N+1} \end{bmatrix} \tag{1-26}$$

Furthermore in Fig. 1-1,

$$B_{N+1} \equiv 0 \tag{1-27}$$

Therefore,

$$r = \frac{B_o}{A_o} = \frac{S_{21}}{S_{11}} \tag{1-28a}$$

$$t = \frac{A_{N+1}}{A_o} = \frac{1}{S_{11}} \tag{1-28b}$$

1-5. EXAMPLES

We have calculated r vs λ for five different refractive index profiles using both the exact multilayer technique and the coupled mode approach. The coupled mode equations (1-13a) and (1-13b) were solved numerically using Runge-Kutta. The results are shown in

Figure 1-2. The multilayer technique gives exact results of course, only if the refractive index is constant within each of the slabs. This will be the case, in the limit, as each of the slab thicknesses go to zero. The solid curves given in Figure 1-2 were obtained by decreasing all the slab thicknesses until further reductions had no appreciable affects upon the multilayer theory predictions. Excellent agreement is seen to exist for the periodic grating but the agreement is poor for the nonperiodic gratings.

Several assumptions have been made in the derivation of the first order coupled mode equations (1-13a) and (1-13b). Gaylord believes that the assumption given by Eq. (1-12) may contribute the most error. [18] Kogelnik has shown that this assumption is justified for sinusoidal gratings, but we feel that his argument is incorrect. Our reasoning goes as follows:

For a sinusoidal grating at the Bragg angle $\Delta\beta(z) \equiv 0$ and $\Delta n(z)$ is a constant. Thus, Eqs. (1-13a) and (1-13b) may be rewritten as

$$A'(z) = KB(z) \tag{1-29a}$$

$$B'(z) = KA(z) \tag{1-29b}$$

where K is a constant. Combining Eqs. (1-29a) and (1-29b) yields

$$A''(z) = K^2 A(z) \tag{1-30}$$

Now for a reflection grating with unslanted fringes $B(D) \equiv 0$ and $A(D) \neq 0$. Thus Eq. (1-29a) implies

$$A'(D) = 0 \tag{1-31}$$

while Eq. (1-30) implies

$$A''(D) \neq 0 \tag{1-32}$$

Therefore,

$$|A''(D)| > |p_z A'(D)| \tag{1-33}$$

which contradicts the assumption of Eq. (1-12) for $z = D$.

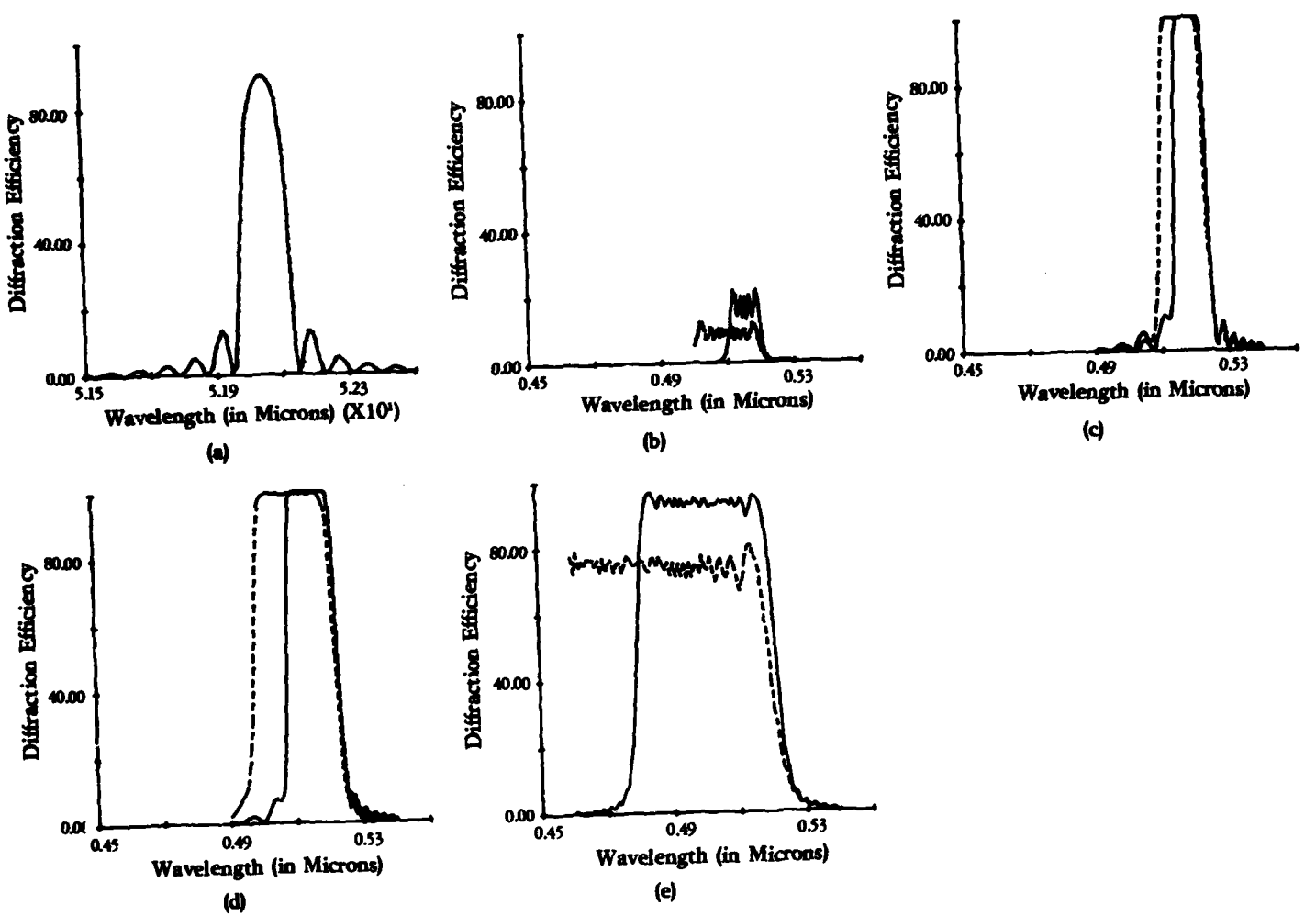

FIGURE 1-2. SOLID CURVE MULTILAYER THEORY, DASHED CURVE COUPLED MODE THEORY. $n(z)=n_0+\Delta n(z)\sin(2\pi f(z)z)$, $\theta_0=0°$, and $D=150\ \mu m$. (a) $\Delta n(z)=0.002$, $f(z)=5.76\ \mu m^{-1}$; (b) $\Delta n(z)=0.002$, $f(z)=(5.76+0.125z/D)\ \mu m^{-1}$; (c) $\Delta n(z)=0.015$, $f(z)=(5.76+0.05z/D)\ \mu m^{-1}$; (d) $\Delta n(z)=0.015$, $f(z)=(5.76+0.125z/D)\ \mu m^{-1}$; (e) $\Delta n(z)=0.015$, $f(z)=(5.76+0.49z/D)\ \mu m^{-1}$

1-6. CONCLUSIONS

We have shown by example that coupled mode theory can give inaccurate results under certain conditions. Furthermore, one of the common assumptions used with coupled mode theory, i.e., neglecting second derivatives, has been shown to lack justification. It appears that great care must be taken when attempting to use coupled mode theory for analyzing optical propagation through gratings and corrugated waveguide filters.

REFERENCES/SECTION 1

1. C. Elachi, "Waves in Active and Passive Periodic Structures: A Review", Proc. of IEEE, 64, No. 12, p. 1666, Dec. 1976.

2. E. C. Titchmarch, Eigenfunction Expansions Associated with Second Order Differential Equations, Part II, Oxford University Press, London, 1958.

3. C. B. Burckhardt, "Diffraction of a Plane Wave at a Sinusoidally Stratified Dielectric Grating", J. Opt. Soc. Am., 56, No. 11, Nov. 1966.

4. A. Yariv, Introduction to Optical Electronics (2nd Ed), Chap. 13, Holt, Rinehart and Winston, New York, 1971.

5. T. Tamir: Editor, Topics in Applied Physics Vol. 7 (Integrated Optics, Chap. 2), Springer-Verlag, New York, 1979.

6. W. H. Louisell, Coupled Mode and Parametric Electronics, John Wiley & Sons, New York, 1960.

7. H. Kogelnik, "Coupled Wave Theory for Thick Hologram Gratings", Bell Sys. Tech. J., 48, No. 9, p.2909, Nov. 1969.

8. R. Magnusson and T. K. Gaylord, "Analysis of Multiwave Diffraction by Thick Gratings", J. Opt. Soc. Am., 67, p. 1165, Sept. 1977.

9. H. Kogelnik, "Filter Response of Nonuniform Almost-Periodic Structures", Bell Sys. Tech. J., 55, No. 1, p. 109, Jan. 1976.

10. D. C. Flanders, H. Kogelnik, R. V. Schmidt, and C. V. Shank, Appl. Phys. Lett., 24, p. 194, Feb. 15, 1974.

11. K. O. Hill, "Optical-Waveguide Band-Rejection Filters: Design" Appl. Opt., 13, No. 2, p. 2886, Dec. 1974.

12. M. Matsuhara, K. O. Hill, and A. Watanabe, "Optical Waveguide Filters: Synthesis", J. Opt. Soc. Am., 65, No. 7, p. 804, July 1975.

13. R. Shubert, "Theory of Optical-Waveguide Distributed Lasers with Nonuniform Gain and Coupling", J. Appl. Phys., 15, No. 1, p. 209, Jan. 1974.

14. Z. Knittl, Optics of Thin Films, (Chap. 2), John Wiley & Sons, New York, 1976.

15. K. Winick, Optical Propagation Through Horizontally Stratified Quasi-Sinusoidal Phase Gratings, Ph.D. Dissertation University of Michigan 1981.

REFERENCES /SECTION 1

16. K. Sakuda and A. Yariv, "Analysis of Optical Propagation in a Corrugated Dielectric Waveguide", Opt. Comm., 8. No. 1, p. 1, May 1973.

17. H. Stoll and Yariv,"Coupled-Mode Analysis of Periodic Dielectric Waveguides", Opt. Comm., 8 No. 1, p.5, May 1973.

18. M. G. Moharam and T. K. Gaylord, "Rigorous Coupled-Wave Analysis of Planar-Grating Diffraction", 71, No. 7, p. 811, July 1981.

Section 2
AN ITERATIVE FOURIER TRANSFORM DESIGN TECHNIQUE

In this section an iterative technique for designing reflection gratings having arbitrary reflectance vs. wavelength (or angle of incidence) characteristics is presented. The technique is based on Fourier transforms and is similar to the multilayer dielectric stack design approaches developed earlier by Delano and Sossi. Reflection grating design, using the iterative technique, is illustrated with two examples. In addition, the reflection grating design technique is shown in Appendix A, to be applicable, with slight modification, to the multilayer dielectric stack design problem.

2.1 INTRODUCTION

Two approaches for determining the reflectivity characteristics of periodic and aperiodic reflection gratings, first order coupled mode theory and Abelès' multilayer theory, were presented in section one. The two approaches were seen to give identical results for sinusoidal gratings but substantially different results for some aperiodic gratings. Recall that Abelès' multilayer theory is known to be exact, whereas first order coupled mode theory is approximate. A formal mathematical analogy between corrugated waveguide filters (CWF) and reflection gratings will be demonstrated in chapter three, thus raising the possibility of applying reflection grating design and analysis techniques to corrugated waveguide filters. It is the aim of this chapter to describe an analytic approach for designing reflection grating filters. The approach allows one to determine the refractive index profile, n(z), which results in some user specified grating reflectivity vs. wavelength characteristic. The reflection gratings to be considered will be structurally identical to those described in section one.

Analytic design techniques for reflection gratings and corrugated waveguide filters have been under investigation during the last ten years. Kogelnik has computed the characteristics of some aperiodic CWF, but has not indicated any approach for designing filters which would have specified reflectivity characteristics.[1] Shubert has demonstrated that step variations in the periodic corrugations of a distributed feedback laser can result in lower threshold gains, greater higher order mode rejection, and unidirectional operation.[2] Matsuhara, et. al. have even proposed a general technique for CWF synthesis.[3] Kogelnik's analysis approach and Matsuhara's analysis and design technique are suspect, since they depend on first order coupled mode theory. Furthermore, even within the framework of first order coupled mode theory, Matsuhara's approach requires one to make several questionable assumptions.

Design techniques for multilayer dielectric filters have been, and are still actively being, investigated. [4-6] The reflection grating design approach, to be described below, relies heavily on multilayer dielectric filter theory. It is quite similar to some of the multilayer dielectric filter Fourier Transform techniques developed by Delano,[7-8] Sossi,[9-11] Pegis,[12] and Knittl[5]. Reference 8 provides an excellent overview of multilayer dielectric filter Fourier synthesis techniques. Greenewalt, et. al. [13] has also developed a Fourier synthesis technique. In Appendix A,our reflection grating design approach is extended to multilayer dielectric filters.

2.2 REFLECTION COEFFICIENT DIFFERENTIAL EQUATION

We start by deriving a differential equation for the reflection coefficient. Consider the pure dielectric shown in Figure 1-1 which has a refractive index variation $n(z)$. The dielectric is assumed to be of infinite extent in both the x and y dimensions. Regions c and s have refractive indices $n_c = n(0)$ and $n_s = n(D)$, respectively. An s polarized (electric field along the y axis) plane wave of wavelength λ is incident at angle of θ_0 upon the dielectric. Some of the incident field is reflected, and the remainder is transmitted. The incident electric field amplitude is designated E_R, while the reflected and transmitted electric field amplitudes are designated E_L and $\tilde{E}_R$, respectively. The reflection and transmission coefficients are defined by Equations (1-3a) and(1-3b).

In all three regions, the total electric (E) and total magnetic (H) field components can be written as

$$E_y(x,z) = U(z)\exp(-i\rho_x x) \qquad (2\text{-}1a)$$

$$H_x(x,z) = V(z)\exp(-i\rho_x x) \qquad (2\text{-}1b)$$

$$H_z(x,z) = W(z)\exp(-i\rho_x x) \qquad (2\text{-}1c)$$

where

$$\rho_x = \frac{2\pi}{\lambda} n(0)\sin\theta_o \qquad (2\text{-}1d)$$

From two of Maxwell's Equations

$$\nabla x\bar{E} = -i\omega\mu(z)\bar{H} \qquad (2\text{-}2a)$$

and

$$\nabla x\bar{H} = \bar{J} + i\omega\varepsilon(z)\bar{E} \qquad (2\text{-}2b)$$

where

$\omega = \frac{2\pi}{\lambda} c$ (c is the speed of light in vacuum)

$\mu(z)$ is the permeability

$\varepsilon(z)$ is the permittivity

it follows that

$$\frac{\partial E_y}{\partial z} = i\omega\mu(z)H_x \qquad (2\text{-}3a)$$

$$\frac{\partial E_y}{\partial x} = -i\omega\mu(z)H_z \qquad (2\text{-}3b)$$

$$\frac{\partial H_x}{\partial z} - \frac{\partial H_z}{\partial x} = i\omega\varepsilon(z)E_y \qquad (2\text{-}3c)$$

Substituting Equations (2-1a) - (2-1c) into Equations (2-3a) - (2-3c) yields

$$U'(z) = i\omega\mu(z)V(z) \qquad (2\text{-}4a)$$

$$-i\rho_x U(z) = -i\omega\mu(z)W(z) \qquad (2\text{-}4b)$$

$$V'(z) + i\rho_x W(z) = i\omega\varepsilon(z)U(z) \qquad (2\text{-}4c)$$

Equations (2-4b) and (2-4c) can be combined to give

$$V'(z) = i\left(-\frac{\rho_x^2}{\omega\mu(z)} + \omega\varepsilon(z)\right)U(z) \qquad (2\text{-}5)$$

The permeability and permittivity of free space will be designated μ_o and ε_o, respectively. The quantities $\theta(z)$, $\gamma(z)$ and $\beta(z)$ are defined below

$$\cos^2\theta(z) \triangleq 1 - \frac{\mu(0)\varepsilon(0)}{\mu(z)\varepsilon(z)} \sin^2 \theta_o \qquad (2\text{-}6a)$$

$$\gamma(z) \triangleq (\mu(z)\varepsilon(z)/\mu_o\varepsilon_o)^{1/2} \cos \theta(z) \qquad (2\text{-}6b)$$

$$\beta(z) \triangleq \sqrt{\mu(z)/\varepsilon(z)}\cos \theta(z) \qquad (2\text{-}6c)$$

$$K \triangleq \frac{2\pi}{\lambda} \qquad (2\text{-}6d)$$

Using the above four definitions, Equations (2-4a) and (2-5) can be rewritten as

$$U'(z) = iK\gamma(z)\beta(z)\, V(z) \qquad (2\text{-}7a)$$

$$V'(z) = iK(\gamma(z)/\beta(z))U(z) \qquad (2\text{-}7b)$$

The input impedance, Q(z) is defined by

$$Q(z) \triangleq \frac{U(z)}{V(z)} \qquad (2\text{-}8)$$

If follows from Equations (2-7a) and (2-7b) that

$$Q'(z) = iK\,\gamma(z)\beta(z) - iK(\gamma(z)/\beta(z))Q^2(z) \qquad (2\text{-}9)$$

Assume that the section of the dielectric to the left of the plane $z = z_o$ ($0 \leq z_o \leq D$) is replaced by a homogeneous dielectric of refractive index $n(z_o)$. Further suppose that an s polarized plane wave, having x propagation constant, ρ_x, and electric field strength E_R, is incident from the left onto the $z = z_o$ plane. A portion of the incident plane wave is reflected and the remainder is transmitted. From Eq. (2-3a) and (2-3b) the incident (i) and reflected (r) plane wave fields can be written as

$$E_{iy}(x,z) = E_R \exp(-i(\rho_x x + \rho_z(z_o)z) \quad (2\text{-}10a)$$

$$H_{ix}(x,z) = -\frac{P_z(z_o)}{\omega\mu(z_o)} E_R \exp(-i(\rho_x x + \rho_z(z_o)z)) \quad (2\text{-}10b)$$

$$H_{iz}(x,z) = \frac{\rho_x}{\omega\mu(z_o)} E_R \exp(-i(\rho_x x + \rho_z(z_o)z) \quad (2\text{-}10c)$$

$$E_{ry}(x,z) = E_L \exp(-i(\rho_x x - \rho_z(z_o)z)) \quad (2\text{-}10d)$$

$$H_{rx}(x,z) = \frac{\rho_z(z_o)}{\omega\mu(z_o)} E_L \exp(-i(\rho_x x - \rho_z(z_o)z)) \quad (2\text{-}10e)$$

$$H_{rz}(x,z) = \frac{\rho_x}{\omega\mu(z_o)} E_L \exp(-i(\rho_x x - \rho_z(z_o)z)) \quad (2\text{-}10f)$$

where

$$\rho_z(z) = +\sqrt{(\frac{2\pi}{\lambda})^2 n^2(z_o) - \rho_x^2} \quad (2\text{-}10g)$$

Continuity of the tangential electric and magnetic field components across the $z = z_o$ plane requires that

$$E_{iy}(x,z_o) + E_{ry}(x,z_o) = U(z_o)\exp(-i\rho_x x) \quad (2\text{-}11a)$$

and

$$H_{ix}(x,z_o) + H_{rx}(x,z_o) = V(z_o) \exp(-i\rho_x x) \quad (2\text{-}11b)$$

Combining Equations (2-10a) through (2-11b) yields

$$\frac{1 + E_L/E_R}{-1 + E_L/E_R} \frac{\omega\mu(z_o)}{\rho_z(z_o)} = \frac{U(z_o)}{V(z_o)} = Q(z_o) \quad (2\text{-}12)$$

But by Equations (2-1d), (2-10g), (2-6a) and (2-6c)

$$\frac{\omega\mu(z_o)}{\rho_z(z_o)} = \beta(z_o) \tag{2-13}$$

Using Equations (2-13) and the definition of the reflection coefficient, r, given by Equation (1-3a), Equation (2-12) can be rewritten as

$$\frac{1 + r(z_o)}{-1 + r(z_o)}\ \beta(z_o) = Q(z_o) \tag{2-14}$$

Finally substituting Equation (2-14) into Equation (2-9) results in the following differential equation for $r(z_o)$

$$r'(z_o) = i2K\gamma(z_o)r(z_o) - \frac{\beta'(z_o)}{2\beta(z_o)}\,(1 - r^2(z_o)) \tag{2-15}$$

Equation (2-15) was originally given by Walker and Wax[14] and Kofink[15]. When $|r(z_o)|^2 \ll 1$, then by Equation (2-15)

$$r'(z_o) \simeq i2K\gamma(z_o)r(z_o) - \frac{\beta'(z_o)}{2\beta(z_o)} \tag{2-16}$$

The solution, r(z), of Equation (2-16) with equality assumed is

$$r(z)\exp(-i2K\int_o^z \gamma(\zeta)d\zeta) - r(o) = -\int_o^z \frac{\beta'(p)}{2\beta(p)}\exp[-2iK\int_o^p \gamma(\zeta)d\zeta]dp \tag{2-17}$$

Imposing the boundary condition r(D) = 0, it immediately follows that

$$r(o) \simeq \int_o^D \frac{\beta'(p)}{2\beta(p)}\exp[-i2K\int_o^p \gamma(\zeta)d\zeta]dp \tag{2-18}$$

The refractive index n(z) is given by

$$n(z) = \sqrt{\frac{\mu(z)\varepsilon(z)}{\mu_o \varepsilon_o}} \tag{2-19}$$

We restrict our analysis to nonmagnetic dielectrics, and therefore,

$$\mu(z) = \mu_o \tag{2-20}$$

The definitions given by Equations (2-6a) - (2-6c) can now be rewritten as

$$\cos^2\theta(z) \triangleq 1 - \frac{n^2(o)}{n^2(z)} \sin^2\theta_o \tag{2-21a}$$

$$\gamma(z) = n(z)\cos\theta(z) \tag{2-21b}$$

$$\beta(z) = \frac{\sqrt{\mu_o/\varepsilon_o}}{n(z)\cos\theta(z)} \tag{2-21c}$$

From Equations (2-21a) and (2-21c)

$$\frac{1}{\beta(z)} \frac{d\beta(z)}{dz} = \frac{n'(z)}{n(z)\cos^2\theta(z)} = \frac{n'(z)}{n(z)\left[1 - \frac{n^2(o)}{n^2(z)} \sin^2\theta_o\right]} \tag{2-22a}$$

$$\int_o^z \gamma(\zeta)d\zeta = \int_o^z n(\zeta)\left[1 - \frac{n^2(o)}{n^2(\zeta)} \sin^2\theta_o\right]^{1/2} d\zeta \tag{2-22b}$$

But by Equations (1-1) and(1-2)

$$\frac{n(o)}{n(\zeta)} \simeq 1 \tag{2-23}$$

and so

$$\frac{1}{\beta(z)}\frac{d\beta(z)}{dz} \simeq \frac{n'(z)}{n_o\cos^2\theta_o} \qquad (2\text{-}24a)$$

$$\int_o^z \gamma(\zeta)d\zeta \simeq \int_o^z n(\zeta)\cos\theta_o d\zeta \simeq n_o(\cos\theta_o)z \qquad (2\text{-}24b)$$

Finally, combining Equations (2-18) with (2-24a) and (2-24b) yields

$$r(o) \simeq \int_o^D \frac{n'(z)}{2n_o\cos^2\theta_o} \exp[-i2Kn_o(\cos\theta_o)z]dz \qquad (2\text{-}25)$$

The reflection coefficient, r(o), times $\cos^2\theta_o$ is a function of $\frac{\cos\theta_o}{\lambda}$ as can be seen from Equation (2-25). There are several places in this section where n(z) is assumed to be of the form given by Equations (1-1) and (1-2). In Appendix A, the results derived in this chapter are extended to n(z) of arbitrary form.

Now divide the structure shown in Figure 1-1 into N slabs each parallel to the x-y plane (see Figure 2-1)

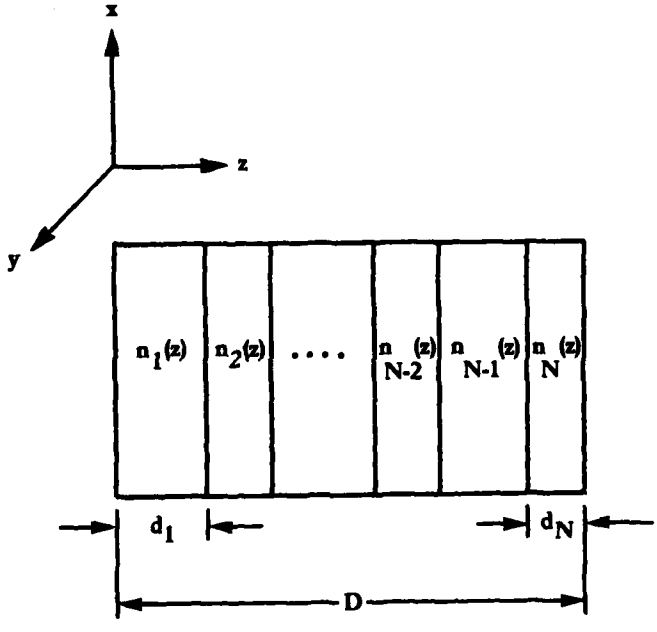

FIGURE 2-1. SLAB DECOMPOSITION

The j^{th} slab has thickness d_j, and refractive index $n_j(z)$ given by

$$n_j(z) \triangleq n(z - \sum_{\ell=1}^{j-1} d_\ell) \quad j \neq 1$$

$$n_1(z) \triangleq n(z) \tag{2-26}$$

Thus, we can write

$$2n_o\cos^2\theta_o\, F(\frac{2\cos\theta_o}{\lambda}) \triangleq \int_o^D n'(z)\exp[-i2Kn_o(\cos\theta_o)z]dz$$

$$= P_1 + \sum_{j=2}^{N} P_j \exp[i2\sum_{\ell=1}^{j-1}\phi_\ell] \tag{2-27a}$$

where

$$P_j \triangleq \int_o^{d_j} n_j(z)\exp[-i2Kn_o(\cos\theta_o)z]dz \tag{2-27b}$$

and

$$\phi_j \triangleq Kn_o(\cos\theta_o)d_j \tag{2-27c}$$

By defining n(z) to be identically zero for z> D and z< 0, we can write

$$2n_o\cos^2\theta_o\, F(\frac{2\cos\theta_o}{\lambda}) = \int_{-\infty}^{\infty} n'(z)\exp[-i2Kn_o(\cos\theta_o)z]dz \tag{2-27d}$$

2.3 TRANSFER MATRIX DEVELOPMENT

Consider a pure dielectric material which has a refractive index variation along the z axis as shown in Figure 2-2.

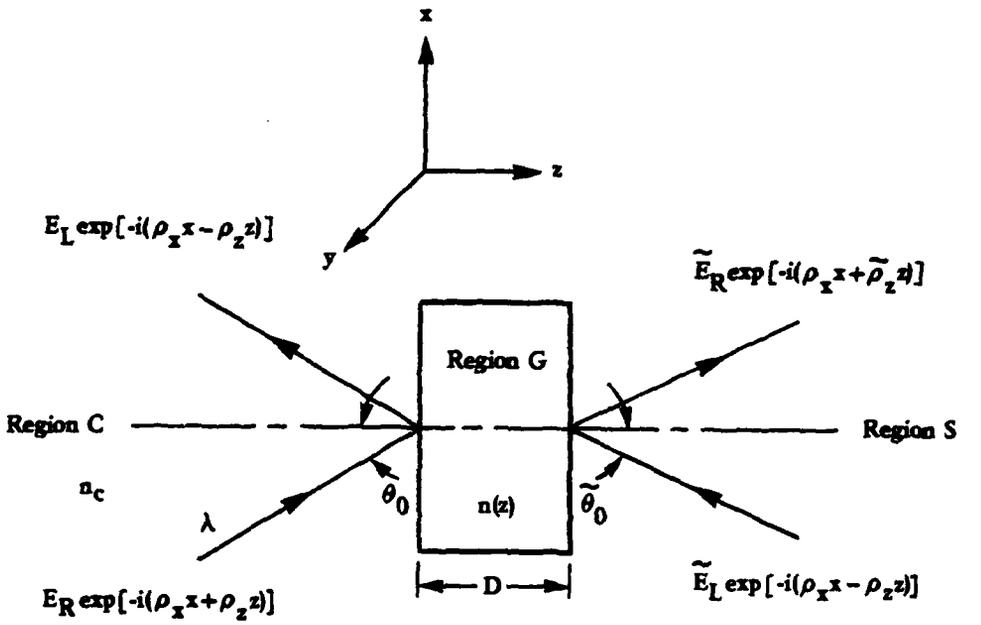

$$\rho_x = \frac{2\pi}{\lambda} n_c \sin\theta_0 = \frac{2\pi}{\lambda} n_s \sin\tilde{\theta}_0$$

$$\rho_x^2 + \rho_z^2 = \left(\frac{2\pi}{\lambda} n_c\right)^2$$

$$\tilde{\rho}_x^2 + \tilde{\rho}_z^2 = \left(\frac{2\pi}{\lambda} n_s\right)^2$$

FIGURE 2-2. DIELECTRIC MATERIAL HAVING A REFRACTIVE INDEX VARIATION IN THE Z DIRECTION. Also shown are two planewave fields at the front and rear surfaces.

If, as indicated in the Figure 2-2, the electric fields on each side of the dielectric material are represented as the sum of the two plane waves propagating in opposite directions, then E_L and E_R can be related to $\tilde{E}_L$ and $\tilde{E}_R$ through a two by two transfer matrix S. The relationship is given explicitly by

$$\begin{bmatrix} E_R \\ E_L \end{bmatrix} = \underbrace{\begin{bmatrix} S_{11} & S_{12} \\ S_{21} & S_{22} \end{bmatrix}}_{S} \begin{bmatrix} \tilde{E}_R \\ \tilde{E}_L \end{bmatrix} \tag{2-28}$$

The right-going reflection and transmission coefficients r and t, respectively, and the left-going reflection and transmission coefficients, $\tilde{r}$ and $\tilde{t}$, respectively, are defined by

$$r = |r|\exp[i\gamma] \triangleq \left.\frac{E_L}{E_R}\right|_{\tilde{E}_L = 0} \tag{2-29a}$$

$$t = |t|\exp[i\Gamma] \triangleq \frac{\tilde{E}_R}{E_R}\bigg|_{\tilde{E}_{L=0}} \tag{2-29b}$$

$$\tilde{r} = |\tilde{r}|\exp[i\tilde{\gamma}] \triangleq \frac{\tilde{E}_R}{\tilde{E}_L}\bigg|_{E_R = 0} \tag{2-29c}$$

$$\tilde{t} = |\tilde{t}|\exp[i\tilde{\Gamma}] \triangleq \frac{E_L}{\tilde{E}_L}\bigg|_{E_R = 0} \tag{2-29d}$$

If follows immediately from Equations (2-28) and (2-29) that

$$r = \frac{S_{21}}{S_{11}} \tag{2-30a}$$

$$t = \frac{1}{S_{11}} \tag{2-30b}$$

$$\tilde{r} = -\frac{S_{12}}{S_{11}} \tag{2-30c}$$

$$\tilde{t} = S_{22} - \frac{S_{12}S_{21}}{S_{11}} \tag{2-30d}$$

and so

$$S_{11} = 1/t \tag{2-31a}$$

$$S_{12} = -\tilde{r}/t \tag{2-31b}$$

$$S_{21} = r/t \tag{2-31c}$$

$$S_{22} = \tilde{t} - \tilde{r}r/t \tag{2-31d}$$

$$S = \frac{1}{t}\begin{bmatrix} 1 & -\tilde{r} \\ r & \tilde{t}t - \tilde{r}r \end{bmatrix} \tag{2-32}$$

Stoke's reversibility theorem [16] requires that

$$t^*\tilde{r} + r^*t = 0 \tag{2-33a}$$

and

$$t^*\tilde{t} + rr^* = 1 \tag{2-33b}$$

where * denotes complex conjugate.

Equation (2-33a) implies

$$\tilde{r} = -r^*\exp[i2\Gamma] \tag{2-34}$$

Combining Equations (2-33b) and (2-34) yields

$$\tilde{t}t - \tilde{r}r = \exp[i2\Gamma] \tag{2-35}$$

Finally, with Equations (2-34) and (2-35), Equation (2-32) becomes

$$S = \frac{1}{t}\begin{bmatrix} 1 & r^*\exp[i2\Gamma] \\ r & \exp[i2\Gamma] \end{bmatrix} \tag{2-36}$$

The matrix S_j is defined by

$$S_j \triangleq \frac{1}{t_j}\begin{bmatrix} 1 & r_j^*\exp[i2\Gamma_j] \\ r_j & \exp[i2\Gamma_j] \end{bmatrix} \tag{2-37}$$

S_j is the transfer matrix associated with the j^{th} dielectric slab shown in Figure 2-1. Thus, the transfer matrix, S, of the entire structure shown in Figure 2-2 is

$$S = \prod_{j=1}^{N} S_j \tag{2-38}$$

Using mathematical induction, it can be shown that[17]

$$\prod_{j=1}^{N} S_j = \prod_{j=1}^{N} \frac{1}{t_j} \begin{bmatrix} C_{11}^{(N)} & C_{12}^{(N)} \\ C_{21}^{(N)} & C_{22}^{(N)} \end{bmatrix} \tag{2-39}$$

where

$$C_{11}^{(N)} = 1 + \text{sum of all ep(m)}, \ \ell_m \leq N \tag{2-40a}$$

$$C_{21}^{(N)} = \text{sum of all op(m)}, \ \ell_m \leq N \tag{2-40b}$$

$$C_{12}^{(N)} = C_{21}^{(N)^*} \exp[i2(\sum_{j=1}^{N} \Gamma_j)] \tag{2-40c}$$

$$C_{22}^{(N)} = C_{11}^{(N)^*} \exp[i2(\sum_{j=1}^{N} \Gamma_j)] \tag{2-40d}$$

and where ep(m) is an expression of the form

$$b_{\ell_1} b_{\ell_2} \ldots b_{\ell_m} \exp[i \sum_{j=0}^{m-1} \sum_{n=\ell_j}^{\ell_{j+1}-1} (1 - (-1)^j)\Gamma_n]$$

$$b_{\ell_j} \triangleq \begin{cases} r_j^* & \text{for j an odd integer} \\ r_j & \text{for j an even integer} \end{cases}$$

$$\ell_o \triangleq 0 \qquad (2\text{-}41a)$$

$$\Gamma_o \triangleq 0$$

m is a positive even integer and $\ell_1, \ell_2 \ldots, \ell_m$ is a monotonically increasing sequence of positive integers

and

op(m) is an expression of the form

$$b_{\ell_1} b_{\ell_2} \ldots b_{\ell_m} \exp\left[i \sum_{j=0}^{m-1} \sum_{n=\ell_j}^{\ell_{j+1}-1} (1 - (-1)^{j+1})\Gamma_n\right]$$

$$b_{\ell_j} \triangleq \begin{cases} r_j & \text{for j an odd integer} \\ r_j^* & \text{for j an even integer} \end{cases}$$

$$\ell_o \triangleq 0 \qquad (2\text{-}41b)$$

$$\Gamma_o \triangleq 0$$

m is a positive odd integer and $\ell_1, \ell_2, \ldots, \ell_m$ is a monotonically increasing sequence of positive integers.

Using Equations (2-30a), (2-30b), (2-39) and (2-40), we can now write

$$r = \frac{C_{21}^{(N)}}{C_{11}^{(N)}} = \frac{\text{sum of all op(m)}, \ \ell_m \leq N}{1 + \text{sum of all ep(m)}, \ell_m \leq N} \qquad (2\text{-}42a)$$

$$t = \frac{1}{C_{11}^{(N)}} = \frac{\left(\prod_{j=1}^{N} t_j\right)}{1 + \text{sum of all ep(m)}, \ \ell_m \leq N} \qquad (2\text{-}42b)$$

$$\frac{r}{t} = \frac{\text{sum of all op(m)}, \ \ell_m \leq N}{\left(\prod_{j=1}^{N} t_j\right)} \qquad (2\text{-}42c)$$

As an example, for N=4 the above three equations become

$$r = \frac{\begin{array}{l} r_1+r_2\exp(i2\Gamma_1) + r_3\exp(i2(\Gamma_1 + \Gamma_2)) + r_4\exp(i2(\Gamma_1+ \Gamma_2 + \Gamma_3)) \\ + r_1r_3^*r_4\exp(i2\,\Gamma_3) + r_2r_3^*r_4\exp(i2(\Gamma_1 + \Gamma_3)) + r_1r_2^*r_3\exp(i2\Gamma_2) \\ + r_1r_2^*r_4\exp(i2(\Gamma_2 + \Gamma_3)) \end{array}}{\begin{array}{l} 1 + r_1^*r_2\exp(i2\Gamma_1) + r_3^*r_4\exp(i2\Gamma_3) + r_1^*r_2r_3^*r_4\exp(i2(\Gamma_1 + \Gamma_3)) \\ + r_2^*r_3\exp(i2\Gamma_2) + r_1^*r_3\exp(i2(\Gamma_1 + \Gamma_2) + r_2^*r_4\exp(i2(\Gamma_2 + \Gamma_3)) \\ + r_1^*r_4\exp(i2(\Gamma_1 +\Gamma_2 +\Gamma_3)) \end{array}}$$

$$t = \frac{t_1t_2t_3t_4\exp(i(\Gamma_1 + \Gamma_2 + \Gamma_3 + \Gamma_4))}{\begin{array}{l} 1 + r_1^*r_2\exp(i2\Gamma_1) + r_3^*r_4\exp(i2\Gamma_3) + r_1^*r_2r_3^*r_4\exp(i2(\Gamma_1 + \Gamma_3)) \\ + r_2^*r_3\exp(i2\Gamma_2) + r_1^*r_3\exp(i2(\Gamma_1 + \Gamma_2)) + r_2^*r_4\exp(i2(\Gamma_2 + \Gamma_3)) \\ + r_1^*r_4\ \exp(i2(\Gamma_1 + \Gamma_2 + \Gamma_3)) \end{array}}$$

$$\frac{r}{t} = \frac{\begin{array}{l} r_1 + r_2\exp(i2\Gamma_1) + r_3\exp(i2(\Gamma_1 + \Gamma_2)) + r_4\exp(i2(\Gamma_1 + \Gamma_2 + \Gamma_3)) \\ + r_1r_3^*r_4\exp(i2\Gamma_3) + r_2r_3^*r_4\exp(i2(\Gamma_1 +\Gamma_3)) + r_1r_2^*r_3\exp(i2\Gamma_2) \\ + r_1r_2^*r_4\exp(i2(\Gamma_2 + \Gamma_3)) \end{array}}{t_1t_2t_3t_4}$$

Formulas analogous to Equations (2-42a) and (2-42b) were first derived for multilayer dielectric stacks by Crook[18]. Equations (2-42) have been exploited, by Pegis[19], Delano[7-8], and Knittl[5] to aid in the design of mulitlayer dielectric stacks and inhomogenous layers.

2.4 THE BASIC DESIGN EQUATION

When $n(z)$ is given by Equations (1-1) and (1-2) and when $|r_j(z_o)|^2 << 1$ for $0 \leq z_o \leq d_j$, then from Equation (2-25)

$$r_j \simeq \int_o^{d_j} \frac{n_j'(z)}{2n_o\cos^2\theta_o} \exp[-i2Kn_o(\cos\theta_o)z]dz \qquad (2\text{-}43)$$

and

$$\tilde{r}_j \simeq \int_{d_j}^{o} \frac{n_j'(d_j - z)}{2n_o\cos^2\theta_o} \exp[-i2Kn_o(\cos\theta_o)(d_j - z)]dz$$

$$= -\exp[-i2Kn_o(\cos\theta_o)d_j] \int_o^{d_j} \frac{n_j'(z)}{2n_o\cos^2\theta_o} \exp[i2Kn_o(\cos\theta_o)z]dz$$

$$\simeq -r_j^* \exp[-i2Kn_o(\cos\theta_o)d_j] \qquad (2\text{-}44)$$

Combining Equations (2-43), (2-44) and (2-34) yields

$$\Gamma_j \simeq -iKn_o(\cos\theta_o)d_j \qquad (2\text{-}45)$$

when $|r_j(z_o)|^2 << 1$, $0 \leq z_o \leq d_j$.

We note that the condition $|r_j(z_o)|^2 << 1$, $0 \leq z_o \leq d_j$ can always be satisfied by choosing d_j sufficiently small.

According to (2-41b),

$$(\text{sum of all op(1)}, \ell_1 \leq N) = r_1 + r_2\exp[i2\Gamma_1] + r_3\exp[i2(\Gamma_1 + \Gamma_2)] + \ldots + r_N\exp[i2(\Gamma_1 + \Gamma_2 + \ldots \Gamma_{N-1})] \qquad (2\text{-}46)$$

Now from Equations (2-43), (2-45), (2-46), and (2-27), it follows that

$$2n_0(\cos^2\theta_0)(\text{sum of all op}(l), \ell_l \leq N) \simeq \int_{-\infty}^{\infty} n'(z)\exp[-2Kn_0(\cos\theta_0)z]dz \tag{2-47}$$

when $|r_j(z_0)|^2 << 1, \quad 0 \leq z_0 \leq d_j$

According to Equation (2-41), op(m) is a product involving an odd number (m) of r_j's. Similarly, ep(m) is a product involving an even number (m) of r_j's. When the d_j's are small, then the r_i's will be small. Thus, we expect |op(m)| and |ep(m)| to decrease rapidly as m increases. If all op(m) and ep(m), m > 1 are neglected then Equation (2-42a) becomes

$$r \simeq \text{sum of all op}(l), \ \ell_l \leq N \tag{2-48a}$$

If all op(m) and ep(m), m > 2 are neglected then Equations (2-42a) and (2-42b) become

$$r \simeq \frac{\text{sum of all op}(l), \ \ell_l \leq N}{1 + \text{sum all ep}(2), \ \ell_2 \leq N} \tag{2-48b}$$

and

$$\frac{r}{t} \simeq \frac{\text{sum of all op}(l), \ \ell_l \leq N}{\left(\prod_{j=1}^{N} t_j\right)} \tag{2-48c}$$

It is expected that Equations (2-48b) and (2-48c) are more accurate than Equation (2-48a) since fewer terms were neglected in their derivation.

Recall that n(z) is linked to op(l) through Equation (2-47). Thus, Equations (2-48a) and (2-48c) can be rewritten as

$$2n_o(\cos^2\theta_o)r \simeq \int_{-\infty}^{\infty} n'(z)\exp[-i2Kn_o(\cos\theta_o)z]dz \qquad (2\text{-}49a)$$

and

$$2n_o(\cos^2\theta_o)\frac{r}{t}\left(\prod_{j=1}^{N} t_j\right) \simeq \int_{-\infty}^{\infty} n'(z)\exp[-i2Kn_o(\cos\theta_o)z]dz \qquad (2\text{-}49b)$$

respectively. Equation (2-48b) appears to be of little use, since a simple expression for the sum of all op(2), $\ell_2 \leq N$ in terms of n(z) is not known. The right hand sides of Equations (2-49a) and (2-49b) are the Fourier transform of n'(z). By the property of Fourier transforms

$$\int_{-\infty}^{\infty} n'(z)\exp[-i2Kn_o(\cos\theta_o)z] = \frac{i2n_o(\cos\theta_o)}{\lambda}\int_{-\infty}^{\infty} n'(z)\exp[-i2Kn_o(\cos\theta_o)z]dz \qquad (2\text{-}50)$$

Using Equation (2-50), noting that n(z) is a real function, and taking the inverse Fourier transform of both sides of Equations (2-49a) and (2-49b), yields

$$n(z) \simeq 2\mathrm{Re}\int_{o}^{\infty} \frac{-i\lambda}{\cos\theta_o}\, r\exp[-2Kn_o(\cos\theta_o)z]d\left(\frac{2n_o\cos\theta_o}{\lambda}\right) \qquad (2\text{-}51a)$$

and

$$n(z) \simeq 2\mathrm{Re}\int_{o}^{\infty} \frac{-i\lambda}{\cos\theta_o}\frac{r}{t}\left(\prod_{j=1}^{N} t_j\right)\exp[-iKn_o(\cos\theta_o)z]d\left(\frac{2n_o\cos\theta_o}{\lambda}\right) \qquad (2\text{-}51b)$$

respectively. In Equations (2-51a) and (2-51b), Re denotes the real part. Equation (2-51a) is only valid in the regime of low reflectivity, i.e. small $|r|^2$, whereas Equation (2-51b) should also be valid in regimes where the reflectivity is not low. Equation (2-51b) is the central result of this chapter and will form the basis of our iterative Fourier Transform reflection grating design technique.

The Fourier Transform relation between r and n(z) for small r, given by Equation (2-51a) is well known[20].

In our design technique, $R \triangleq |r|^2$, is assumed to be given as a function of $\frac{\cos\theta_o}{\lambda}$, and the objective is to find the refractive index, n(z), which results in this R vs. $\frac{\cos\theta_o}{\lambda}$ characteristic. Since $n_c \simeq n_s$ (see Figure (1-1))energy conservation dictates that

$$|r|^2 + |t|^2 \simeq 1 \qquad (2\text{-}52)$$

Thus, Equation (2-51b) can be rewritten as

$$n(z) \simeq 2\mathrm{Re}\int_0^\infty -\left(\frac{R}{1-R}\right)^{1/2} \frac{i\lambda}{\cos\theta_o}\alpha\left(\prod_{j=1}^{N}|t_j|\right)\exp[i2Kn_o\cos\theta_o)z]d\left(\frac{2n_o\cos\theta_o}{\lambda}\right) \qquad (2\text{-}53)$$

where

$$\alpha = \exp[i(\gamma - \Gamma + \sum_{\ell=1}^{N}\Gamma_\ell)] \quad \text{(See Equations (2-29))} \qquad (2\text{-}54a)$$

$$= \exp[i(\gamma - \Gamma - Kn_o(\cos\theta_o)D] \quad \text{(See Equation (2-45) and Figure (2-1))} \qquad (2\text{-}54b)$$

γ and Γ are the phases of the reflection (r) and transmission (t) coefficients, respectively. Also note that α is a function of $\frac{\cos\theta_o}{\lambda}$. In general, R vs. $\frac{\cos\theta_o}{\lambda}$ will be specified by the design, and α vs. $\frac{\cos\theta_o}{\lambda}$ will not be specified.

Our design procedure goes as follows:

1. A refractive index, n(z), is chosen.
2. α is assumed to be identically 1.

Iteration Process

3. Using Abelè's multilayer theory, the t_j's are computed from n(z).
4. n(z) is calculated from Equation (2-53).
5. The corresponding R vs. $\cos\theta_o/\lambda$ characteristic is computed.
6. Step 3 is repeated until n(z) changes little from one iteration to the next.

7. The resulting n(z) is the desired design.

2.5 DESIGN EXAMPLES

The procedure outlined above was used to design two reflection grating filters. The first filter was specified as having the reflectance vs. wavelength characteristics shown in Figure [2-3a], while the second filter was specified as having the characteristic shown in Figure [2-3b]. The evolution of the designs, as a function of the number of iterations, is shown in Figures [2-4 and 2-6]. Given in Figure [2-5] is the refractive index profile corresponding to the last iteration shown in Figure [2-4]. Similarly Figure [2-7] gives the refractive index profile corresponding to the last iteration shown in Figure [2-6]. The refractive index profile is displayed by plotting both $\Delta n(z)$ (solid curve) and f(z) (dashed curve) as a function of z. For both designs, $n_0 = 1.5$, grating thickness = 180 μm, and $\theta_n = 0°$. The initial choice of n(z) for both filters one and two was

$$n(z) = 1.5 + 0.015 \sin 2\pi(5.88\mu m^{-1})z$$

An examination of the points plotted in Figures [2-4] and [2-5] would indicate that both f(z) and $\Delta n(z)$ are essentially constant over intervals of length 1/f(z). Thus, n(z) is simply a sinusoid whose frequency and amplitude are slowly changing as a function of z. The frequency "spikes" shown in Figure [2-7] occur at points where $\Delta n(z) = 0$. Thus, these spikes correspond to spacers (i.e., regions where $\Delta n(z) \simeq 0$) of length 1/(fz).

Although a detailed description of the computer implementation of Equation (2-53) is not provided in this report, some important points

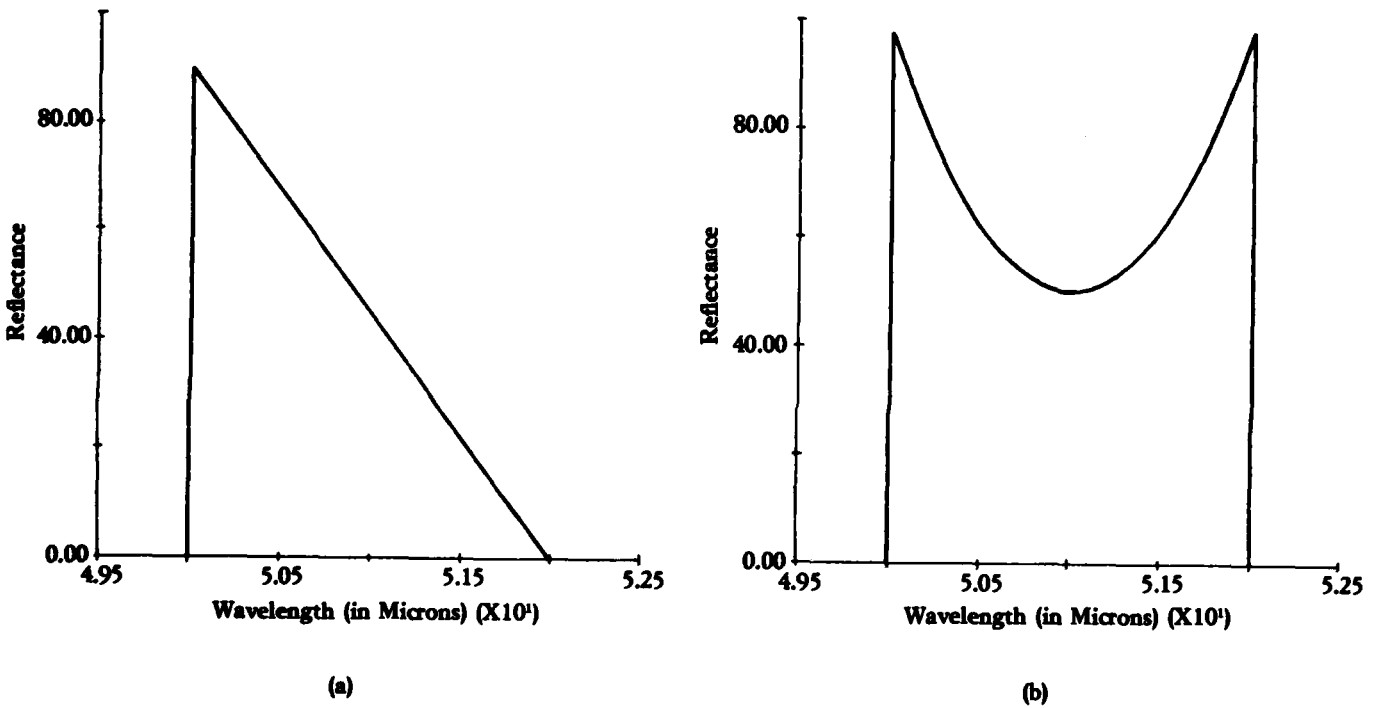

FIGURE 2-3. TWO DESIRED REFLECTANCE VS. WAVELENGTH CHARACTERISTICS: (a) Triangular and (b) Saddle

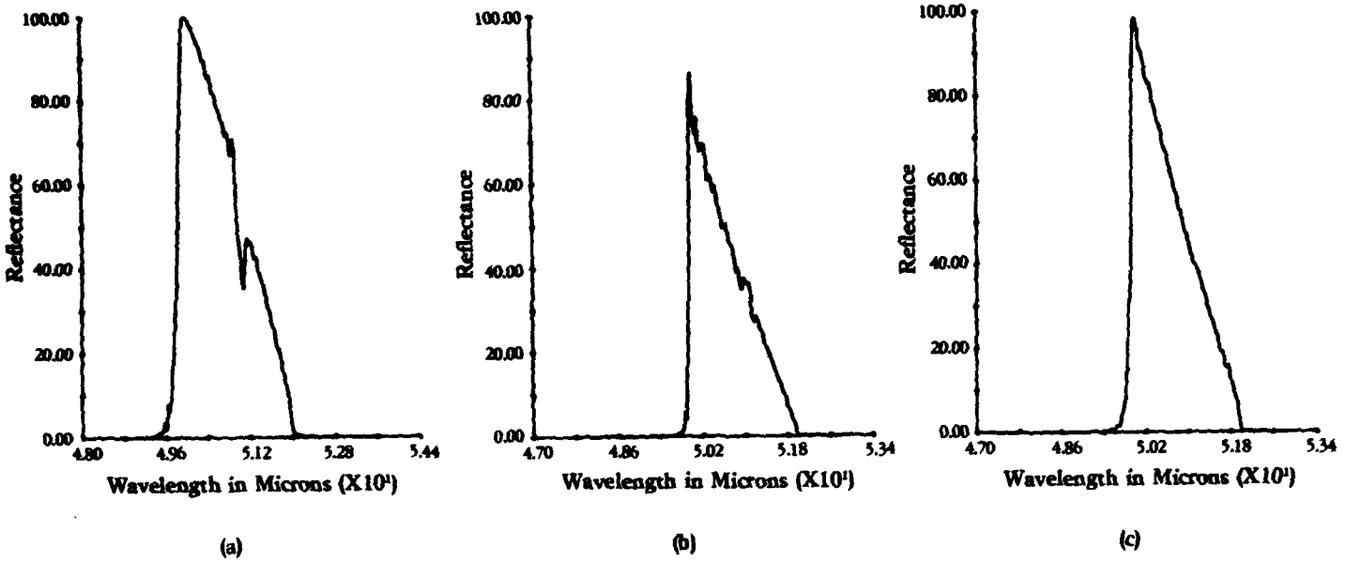

FIGURE 2-4. ITERATIVE FOURIER SYNTHESIS OF A GRATING HAVING A TRIANGULAR CHARACTERISTIC: (a) First Iteration, (b) Second Iteration, and (c) Third Iteration

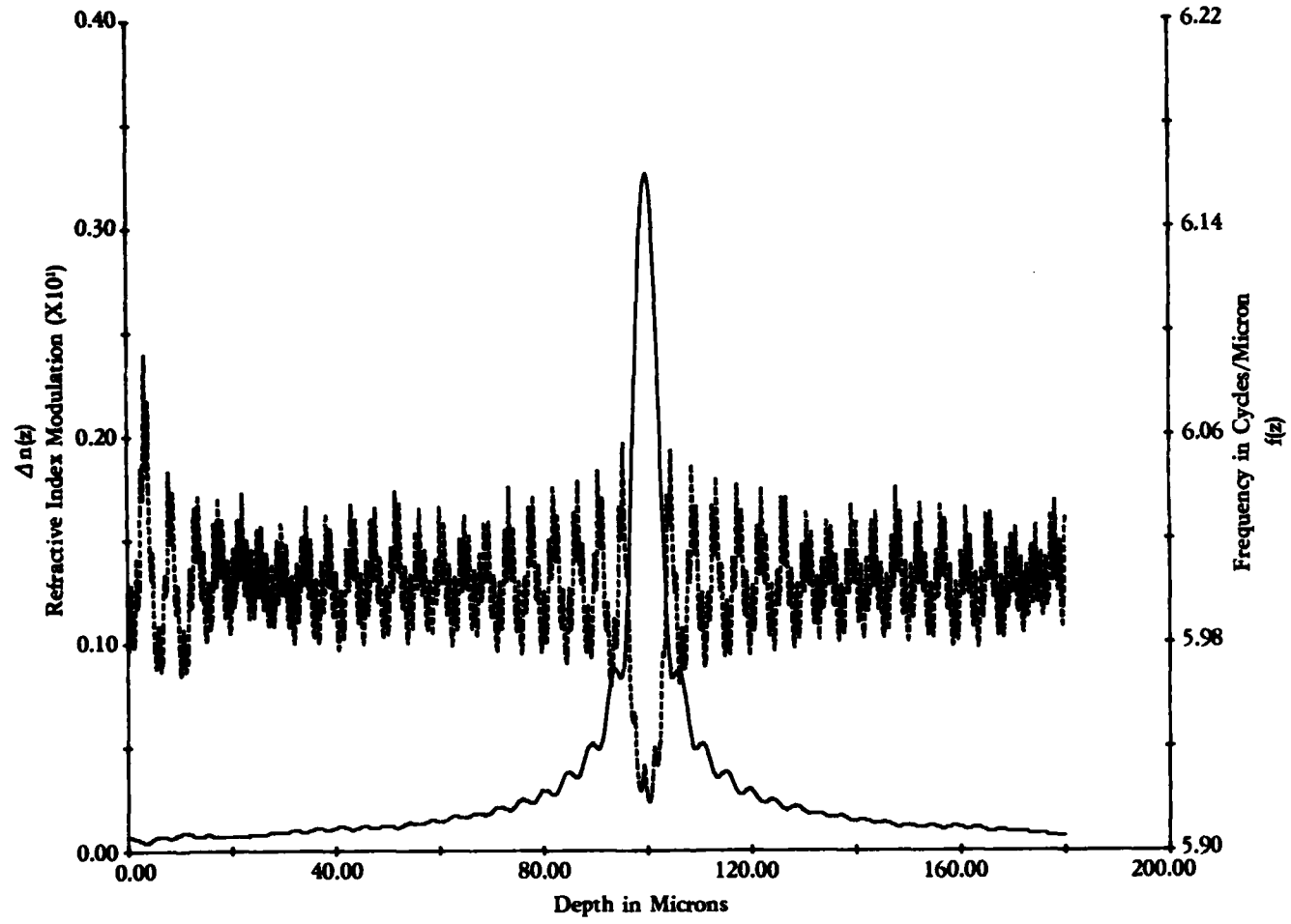

FIGURE 2-5. REFRACTIVE INDEX PROFILE OF A GRATING HAVING A TRIANGULAR CHARACTERISTIC. Solid Curve is $\Delta n(z)$ and Dashed Curve is $f(z)$.

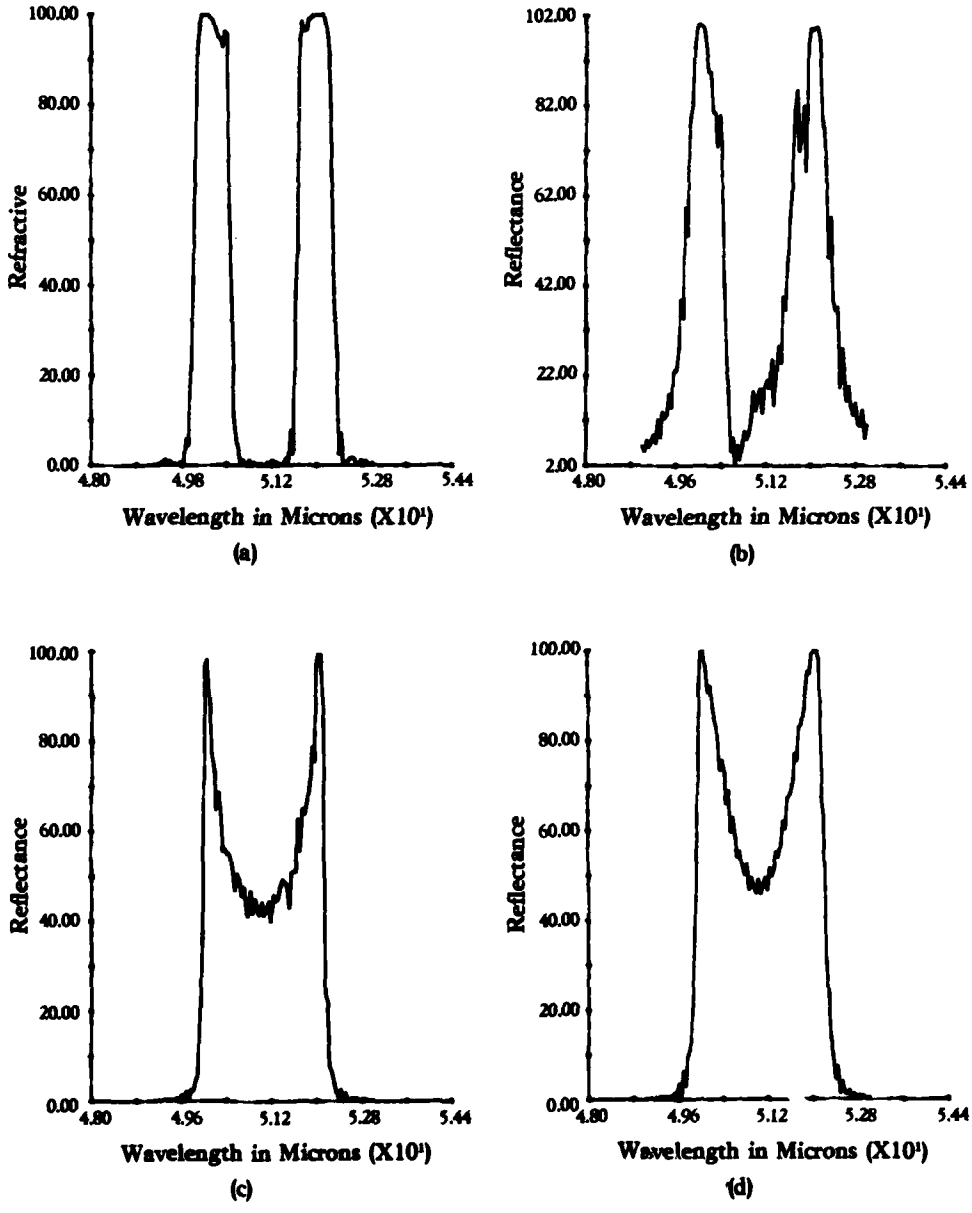

FIGURE 2-6. ITERATIVE FOURIER SYNTHESIS OF A GRATING HAVING A SADDLE CHARACTERISTIC: (a) First Iteration, (b) Second Iteration, (c) Third Iteration, and (d) Fourth Iteration

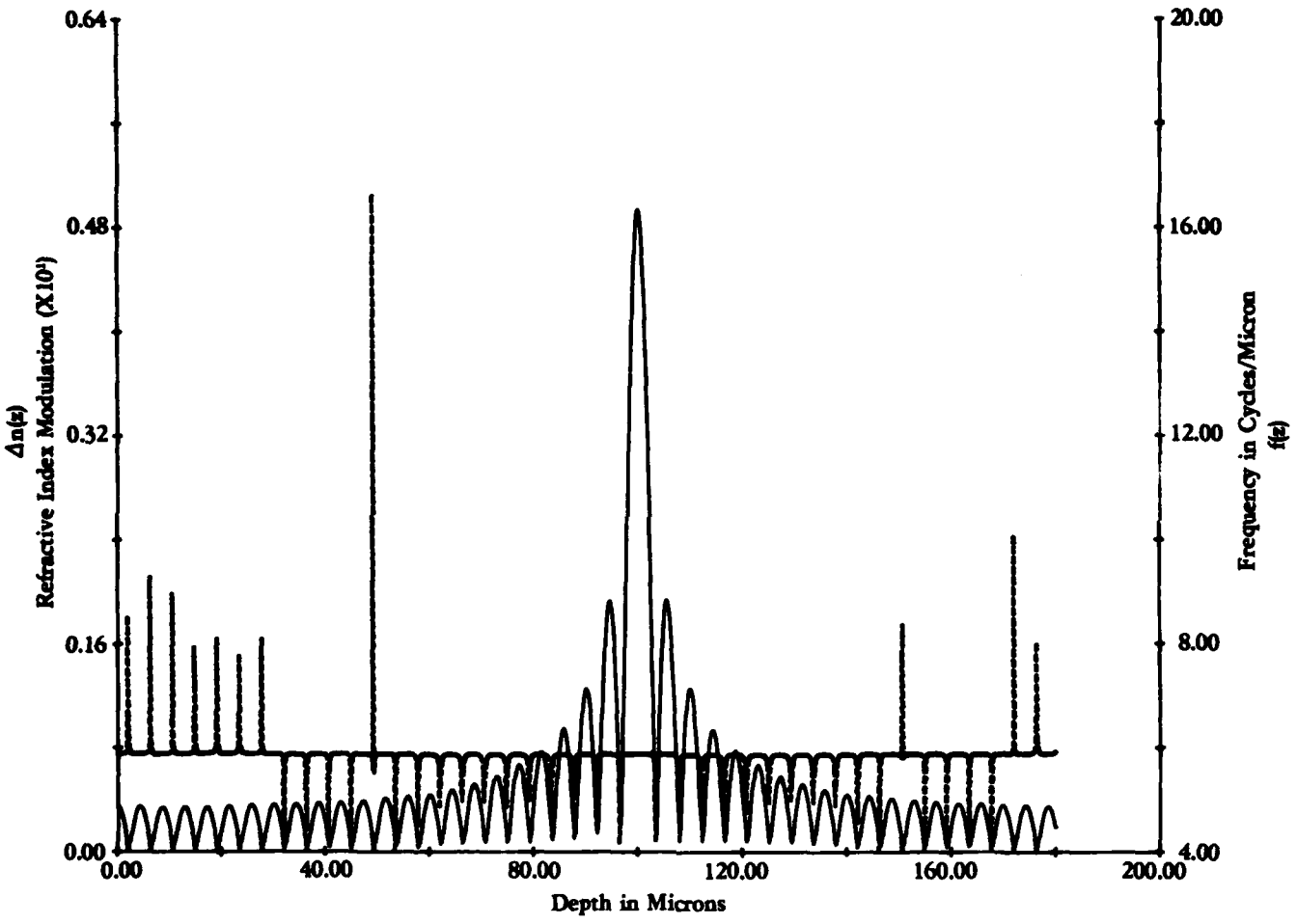

FIGURE 2-7. REFRACTIVE INDEX PROFILE OF A GRATING HAVING A SADDLE CHARACTERISTIC. Solid Curve is $\Delta n(z)$ and Dashed Curve is $f(z)$.

associated with this implementation will be discussed. First, it is noted that the n(z) obtained from Equation (2-53) will be of infinite extent in z. After each iteration, one must truncate the extent of n(z), so that $\Delta n(z)$ is nonzero only over the interval of finite length corresponding to the filter thickness. Generally $\Delta n(z)$ is quite small for large values of z, and thus, little accuracy is lost by the truncation. Second, in order to compute $\prod_{j=1}^{N} |t_j|$, the thickness, d_j of each slab must be chosen. The approximations used in the derivation Equation (2-53) are sensitive to these d_j's. In our designs, for each value of $\cos \theta_o/\lambda$ at which

$$\left(\frac{R}{1-R}\right)^{1/2} \prod_{j=1}^{N} |t_j|$$

was evaluated, d_j was chosen so that $|t_j|^2 \simeq 0.075$. Thus, the d_j's are not fixed during the design of a given filter, but change for each value of $\cos \theta_o/\lambda$. The optimum choice for the d_j's has not been determined. Third, the t_j's associated with each iteration and the resulting R of the final design, are evaluated using an efficient computer implementation of Abelès' multilayer matrix technique. Details of this implementation can be found elsewhere[17]. At each iteration an n(z) is known, and so, Abelès' multilayer matrix technique can be used to determine γ and Γ, and hence α . Thus, it is noted that a better design would most likely be obtained by computing α at each iteration rather than assuming that α is identically one.

APPENDIX/SECTION 2

In this appendix, the reflection grating design technique is extended so as to be applicable to multilayer dielectric stack design. The multilayer dielectric stack design problem consists of two phases. First, the refractive index profile, n(z), required to realize a specified reflectance vs. wavelength characteristic at a fixed angle of incidence, is determined. Second, a discontinuous profile, which could be physically realized by a multilayer dielectric stack, is fitted to the continuous refractive index profile, n(z). The discussion here is restricted to the first phase of the above mentioned design problem. The technique for determining n(z) given the reflectance vs. cos θ_o/λ has already been developed in section two. This technique, however, required n(z) to be of the form given by Equations (1-1) and (1-2). We will remove this restriction below and allow for arbitrary n(z). The extension to arbitrary n(z) involves only a small modification of our reflection grating design technique and so our discussion will be brief.

Repeated below is Equation (2-18) which it will be recalled is valid for arbitrary n(z) provided that $|r(z)| \ll 1$, $0 \leq z \leq D$.

$$r(o) \simeq \int_o^D \frac{\beta'(p)}{2\beta(p)} \exp[-i2K \int_o^P \gamma(\zeta)d\zeta]dp \qquad (2\text{-}18)$$

where

$$\gamma(z) \triangleq n(z)\cos\,\theta(z) \qquad (2\text{-}21b)$$

$$\beta(z) \triangleq \frac{\sqrt{\mu_o/\epsilon_o}}{n(z)\cos\,\theta(z)} \qquad (2\text{-}21c)$$

Next, η is defined by

$$\eta \triangleq 2\int_0^Z \gamma(\zeta)d\zeta \tag{A-1}$$

It is noted that $\eta(z_o)$ is twice the optical path length that a plane wave travels into the dielectric in order to reach the plane $z = z_o$. Combining Equations (2-18), (2-21b) and (2-21c) yields

$$r(o) \simeq \int_0^L \frac{\bar{n}'(\eta)}{2\bar{n}(\eta)\cos^2\bar{\theta}(\eta)} \exp[-ik\eta]d\eta \tag{A-2}$$

where

$$L \triangleq 2\int_0^D \gamma(\zeta)d\zeta \tag{A-3}$$

$$\left.\begin{aligned} \bar{n}(\eta) &\triangleq n(z) \\ \text{and} \qquad & \qquad \eta \text{ and } z \text{ are related via Equation (A-1)} \\ \bar{\theta}(\eta) &\triangleq \theta(z) \end{aligned}\right\} \tag{A-4}$$

Thus, $\bar{n}(\eta)$ and $\bar{\theta}(\eta)$ are simply the refractive index and propagation angle, respectively, expressed as a function of twice the optical path.

$C(\eta)$ and F are defined by

$$C(\eta) \triangleq \frac{\bar{n}'(\eta)}{2\bar{n}(\eta)\cos^2\bar{\theta}(\eta)} = \frac{\bar{n}(\eta)\bar{n}'(\eta)}{2(\bar{n}^2(\eta) - n^2(0)\sin^2\theta(0))} \tag{A-5}$$

$$F \triangleq \int_0^L C(\eta)\exp[-ik\eta]d\eta \tag{A-6}$$

It follows immediately from Equations (A-5) and (A-6) that

$$F = P_1 + \sum_{j=2}^{N} P_j \exp[i \sum_{m=1}^{j-1} \phi_m] \qquad (A-7)$$

where

$$\sum_{j=1}^{N} d_j = L \qquad (A-8)$$

$$P_j \triangleq \int_0^{d_j} C(\eta)\exp[-iK\eta]d\eta \qquad (A-7)$$

$$\phi_j \triangleq Kd_j \qquad (A-10)$$

Using Equation (A-2) it is easy to show (see for instance Equations (2-43) and (2-44)) that

$$\tilde{r}_j \simeq - r_j^* \exp[-iKd_j] \qquad (A-11)$$

Combining Equations (A-11) and (2-34) now yields

$$\Gamma_j \simeq - iKd_j/2 \qquad (A-12)$$

From Equations (2-46), (A-12) and (A-7) - (A-9)

$$F \simeq \text{sum of all } op(1), \ell_1 \leq N \qquad (A-13)$$

From Equations (A-13), (A-6) and (2-48c) it follows that

$$\left(\frac{r}{t} \prod_{j=1}^{N} t_j\right) \simeq \int_{-\infty}^{\infty} C(\eta)\exp[-iK\eta]d\eta \qquad (A-14)$$

Where $C(\eta)$ is defined to be identically zero for $\eta < 0$ or $\eta \geq L$. Delano[7-8] derives an expression similar to Equation (A-14), but assumes as a first order approximation that

$$\prod_{j=1}^{N} t_j \simeq 1$$

From Equation (A-14)

$$C(\eta) = 2Re \int_0^{\infty} \frac{r}{t} \left(\prod_{j=1}^{N} t_j \right) \exp[-iK\eta] d\left(\frac{1}{\lambda}\right) \qquad \text{(A-15)}$$

where r and t are specified as a function of $1/\lambda$ and the t_j's are computed as a function of $1/\lambda$. Note that Equation (A-15) is analogous to Equation (2-51b). Once $C(\eta)$ is computed from Equation (A-15), the differential equation defined by (A-5) can be solved, numerically, to obtain $\bar{n}(\eta)$.

This differential equation can be solved analytically for the case of normal incidence, i.e. $\theta(o) \simeq 0$. Finally, $\bar{n}$ is obtained from n by using the following relationship

$$n\left(\int_0^{\eta} \frac{d\zeta}{\bar{n}(\zeta)\cos\,\bar{\theta}(\zeta)} \right) = \bar{n}(\eta) \qquad \text{(A-16)}$$

or equivalently (see Equation (2-6a))

$$n\left(\int_0^{\infty} \frac{d\zeta}{[\bar{n}^2(\zeta) - n^2(o)\sin^2\theta(o)]^{1/2}} \right) = \bar{n}(\eta) \qquad \text{(A-17)}$$

We note that Equation (A-15) can be rewritten as

$$C(\eta) \simeq 2Re \int_0^{\infty} \left(\frac{R}{1-R}\right)^{1/2} \alpha \prod_{j=1}^{N} |t_j| \exp(iK\eta) d\left(\frac{1}{\lambda}\right) \qquad \text{(A-18)}$$

where

$$\alpha = \exp[i(\gamma - \Gamma + \sum_{j=1}^{N} \Gamma_j)] \qquad \text{(A-19)}$$

Equation (A-18) is analogous to Equation (2-53).

Delano [8] distinguishes between two types of synthesis problems, ones where R is given (first type), and ones where r/t is given (second type). He handles these two types of problems differently. We handle synthesis problems of the first type via Equation (A-15) and those of the second type via Equation (A-18). Thus, it is seen that our technique draws little distinction between the two types of synthesis problems. Sossi [9] derives an equation similar to Equation (A-18) for the case of normal incidence (i.e., $\theta_o = 0$). In his equation the quantity $\prod_{j=1}^{N} t_j$ is replaced by $(1 - \frac{R}{2})^{1/2}$. We have been unable to follow his derivation. Implicit in our derivation, in this appendix, has been the assumption that the refractive index, n(z), does not have discontinuities at the boundaries z = 0 and z = D (i.e., $n_c = n(o)$ and $n_s = n(D)$). We believe that our technique can be modified to remove this restriction. It is also noted that our technique can be easily extended to handle the case of p, rather than s, polarization.

REFERENCES /SECTION 2

[1]. H. Kogelnik, "Filter Response of Nonuniform Almost-Periodic Structures," Bell Sys. Tech. J., 55 No. 1, p. 109, Jan 1976.

[2]. R. Shubert, "Theory of Optical-Waveguide Distributed Lasers with Nonuniform Gain and Coupling," J. Appl. Phys., 15, No. 1, p. 209, Jan 1974.

[3]. M. Matsuhara, K. O. Hill, and Q. Watanabe, "Optical Waveguide Filters: Synthesis," J. Opt. Soc. Am., 65, No. 7, July 1975.

[4]. E. Wolf Ed., Progress in Optics, Vol. VII, Chap. 2 (Methods of Synthesis for Dielectric Multilayer Filters), John Wiley & Sons, New York, 1969.

[5]. Z. Knittl, Optics of Thin Films, John Wiley & Sons, New York, 1976.

[6] H. Kaiser and C. Kaiser, "Mathematical Methods in the Synthesis and Identification of Thin Film Systems," Appl. Optics, 20, No. 1, January, 1981.

[7]. E. Delano, "Fourier Synthesis of Multilayer Filters", 57, No. 12, December, 1967.

[8]. E. Delano, Ph.D. thesis, University of Rochester, June 1966.

[9]. L. Sossi, "A Method For Synthesis of Multilayer Dielectric Interference Coatings," Eesti NSV Tead. Akad. Toim. Fuus. Mat., 23, p. 229 (1974); an English translation of this paper is available from the Translation Services of the Canada Institute for Scientific and Technical Information, National Research Council, Ottawa, Ontario, Canada K1A OS2.

[10]. L. Sossi, "On The Theory of the Synthesis of Multilayer Dielectric Light Filters," Eesti NSV Tead. Akad. Toim. Fuus. Mat., 25, p. 171 (1976), see Ref. 9.

[11]. J. A. Dobrowolski and D. Lowe, "Optical Thin Film Synthesis Program Based on the Use of Fourier Transforms," Appl. Optics, 17, No. 19, p. 3039, October 1978.

[12]. Unpublished.

[13]. C. H. Greenewalt, W. Brandt, and D. D. Friel, "Irridescent Colors of Hummingbird Feathers," J. Opt. Soc. Am., 50, p. 1005, October 1960.

[14]. L. R. Walker and N. Wax, "Non-Uniform Transmission Lines and Reflection Coefficients," J. Appl. Phys., 17, p. 1043, December 1946.

[15]. W. Kofink, "The Reflection of E.M. Waves at an Inhomogeneous Sheet," Ann. Physik, 1, p. 119, 1947.

[16]. I. Santavy, "On the Reversibility of Light Beams in Conducting Media," Opt. Acta, 8, p. 301, November 1961.

[17]. K. A. Winick, Optical Propagation Through Quasi-Sinusoidal, Horizontally Stratified, Phase Gratings, Ph.D. Thesis University of Michigan, 1981.

[18]. A. W. Crook, "The Reflection and Transmission of Light by Any System of Parallel Isotropic Films," J. Opt. Soc. Am., 38, No. 11, p. 954, November 1948.

[19]. R. J. Pegis, "An Exact Design Method for Multilayer Dielectric Films", J. Opt. Soc. Am., 51, No. 11, p. 1255, November 1961.

[20]. See Chapter 10 of reference 5.

Section 3

CORRUGATED WAVEGUIDE FILTERS

A formal mathematical analogy between reflection gratings and corrugated waveguide filters (CWF) is demonstrated in this chapter. The possibility of designing CWF, using the iterative Fourier transform technique developed in Section 2, is explored.

3-1. INTRODUCTION

In this section we demonstrate a formal mathematical analogy between reflection gratings and corrugated waveguide filters (CWF). The development given by Yariv [1] is closely followed. We emphasize that the mathematics developed for CWF are not rigorous. Consequently, predicted results should be experimentally verified and attempts should be made to develop a rigorous mathematical approach.

3-2. FORMAL MATHEMATICAL ANALOGY BETWEEN REFLECTION GRATINGS AND CWF

Consider the CWF shown in Figure [3-1]. The filter consists of a thin waveguiding layer ($0 \leq x \leq a$) of refractive index n_g sandwiched between two dielectrics having refractive indices n_c and n_s ($n_g > n_s > n_c$). The upper surface of the waveguiding layer has a corrugation of small, maximum depth (i.e., $h_o << a$). The refractive index, $n(x, z)$, can be written as

$$n^2(x, z) = n_b^2 + w(x, z)(n_c^2 - n_g^2) \sin 2\pi f(z)z \qquad (3\text{-}1)$$

where n_b equals n_c in region C, n_g in region G and n_s in region S, and where $w(x, z)$ is a binary function which assumes either the value zero or one. Note that $w(x, z) \equiv 0$ for

$$x < 0 \quad \text{or} \quad x > a$$

If we restrict our discussion to transverse electric fields, then Maxwell's wave equation in all three regions can be written as

$$\nabla^2 E_y(x, z) + \left(\frac{2\pi}{\lambda}\right)^2 n^2(x, z) E_y(x, z) = 0 \qquad (3\text{-}2a)$$

or equivalently

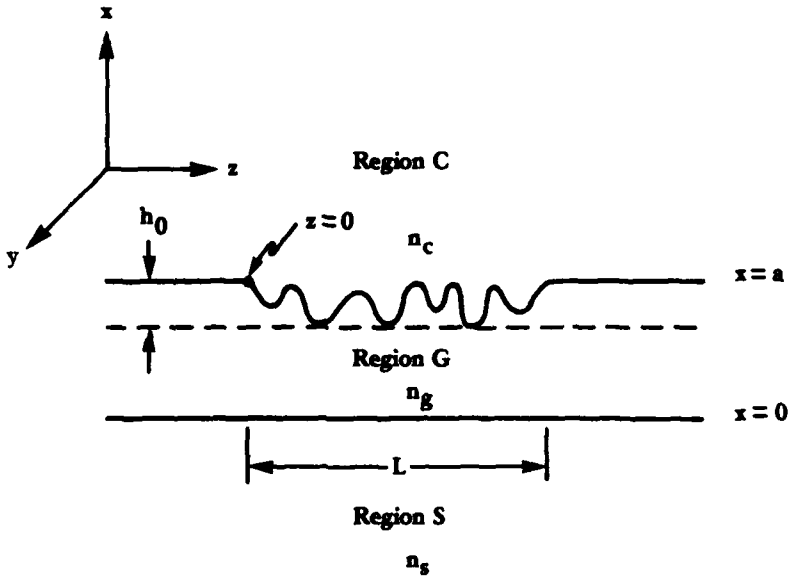

FIGURE 3-1. CORRUGATED WAVEGUIDE FILTER (CWF)

$$\nabla^2 E_y(x, z) + \left(\frac{2\pi}{\lambda}\right)^2 n_b^2 E_y(x, z) + \left(\frac{2\pi}{\lambda}\right)^2 w(x, z)(n_c^2 - n_g^2) \sin(2\pi f(z)z) = 0 \tag{3-2b}$$

Since the corrugation depth is small, we will assume that the total field in the "perturbed" waveguide can be approximately written as the superposition of the confined modes of the waveguide without the corrugation, i.e.,

$$E_y(x, z) \simeq \sum_m A^{(m)}(z) E_y^{(m)}(x) \exp\left[-i\rho_z^{(m)} z\right] + B^{(m)}(z) E_y^{(m)}(x) \exp\left[i\rho_z^{(m)} z\right] \tag{3-3}$$

In Eq. (3-3), $E_y^{(m)}(x) \exp\left[\pm i\rho_z^{(m)} z\right]$ is the m^{th} confined mode of the uncorrugated waveguide. Thus

$$\nabla^2\left[E_y^{(m)}(x) \exp\left[\pm i\rho_z^{(m)} z\right] + \left(\frac{2\pi}{\lambda}\right)^2 n_g^2 E_y^{(m)}(x) \exp\left[\pm i\rho_z^{(m)} z\right]\right] = 0 \tag{3-4}$$

and $\rho_z^{(m)}$ is the propagation constant of the m^{th} mode and can be written as

$$\rho_z^{(m)} = \frac{2\pi}{\lambda} n_g \cos\theta_g^{(m)}(\lambda) \tag{3-5}$$

where $\theta_g^{(m)}(\lambda)$ is the propagation angle of the m^{th} mode within the guiding layer. Note that $\theta_g^{(m)}$, $\rho_z^{(m)}$ and $E_y^{(m)}$ are all functions of λ. Given the geometry of the uncorrugated waveguide, $\theta_g^{(m)}$, $\rho_z^{(m)}$ and $E_y^{(m)}$ are easily determined [1]. For the sake of simplicity the waveguide will be assumed

to be single mode. Equation (3-3) now reduces to

$$E_y(x, z) \simeq A^{(1)}(z)E_y^{(1)}(x) \exp [-i\rho_z^{(1)}z] + B^{(1)}(z)E_y^{(1)}(x) \exp [i\rho_z^{(1)}z] \tag{3-6}$$

The reflection and transmission coefficients r and t of the CWF are defined as $B^{(1)}(0)/A^{(1)}(0)$ and $A^{(1)}(L)/A^{(1)}(0)$ respectively. A simple physical argument indicates that $B^{(1)}(L) \equiv 0$. Substituting Eq. (3-6) into Eq. (3-2b), and then using Eq. (3-4), yields

$$A^{(1)"}(z)E_y^{(1)}(x) \exp [-i\rho_z^{(1)}z] - 2i\rho_z^{(1)}A^{(1)'}(z)E_y^{(1)}(x) \exp [-i\rho_z^{(1)}z]$$

$$+ B^{(1)"}(z)E_y^{(1)}(x) \exp [i\rho_z^{(1)}z] + 2i\rho_z^{(1)} B^{(1)'}(z)E_y^{(1)}(x) \exp [i\rho_z^{(1)}z]$$

$$= -\left(\frac{2\pi}{\lambda}\right)^2 w(x, z)(n_c^2 - n_g^2) \sin \left(2\pi f(z)z\right)\left[A^{(1)}(z)E_y^{(1)}(x) \exp (-i\rho_z^{(1)}z)\right.$$

$$\left. + B^{(1)}(z)E_y^{(1)}(x) \exp (i\rho_z^{(1)}z)\right] \tag{3-7}$$

Now it will be assumed that $E_y^{(1)}(x)$ has been normalized so that

$$\int_{-\infty}^{\infty} \left[E_y^{(1)}(x)\right]^2 dx = 1 \tag{3-8}$$

Furthermore, since the maximum corrugation depth, h_0, is small compared to the thickness, a, of the waveguiding layer

$$E_y^{(1)}(x) \approx E_y^{(1)}(a) \quad \text{for} \quad w(x, z) \neq 0 \tag{3-9}$$

Multiplying both sides of Eq. (3-7) by $E_y^{(1)}(x)$ and then integrating from $-\infty$ to ∞ yields

$$\begin{aligned} &A^{(1)''}(z) \exp [-i\rho_z^{(1)} z] - 2i\rho_z^{(1)}(z) A^{(1)'}(z) \exp [i\rho_z^{(1)} z] \\ &+ B^{(1)''}(z) \exp [i\rho_z^{(1)} z] + 2i\rho_z^{(1)} B^{(1)'}(z) \exp [i\rho_z^{(1)} z] \\ &\approx -\left(\frac{2\pi}{\lambda}\right)^2 (n_c^2 - n_g^2) A^{(1)}(z) \sin (2\pi f(z) z) \exp (-i\rho_z^{(1)} z) \left[E_y^{(1)}(a)\right]^2 \int_{-\infty}^{\infty} w(x, z)\, dx \\ &- \left(\frac{2\pi}{\lambda}\right)^2 (n_c^2 - n_g^2) B^{(1)}(z) \sin (2\pi f(z) z) \exp (i\rho_z^{(1)} z) \left[E_y^{(1)}(a)\right]^2 \int_{-\infty}^{\infty} w(x, z)\, dx \end{aligned} \tag{3-10}$$

where we have used Eqs. (3-8) and (3-9). Recall that $E_y^{(1)}(a)$ is a function of λ. The functions $e(\lambda)$ and $h(z)$ are defined by

$$e(\lambda) \overset{\Delta}{=} \left[E_y^{(1)}(a)\right]^2 \tag{3-11}$$

and

$$h(z) \triangleq \int_{-\infty}^{\infty} w(x, z)\, dz \tag{3-12}$$

Observe that h(z) is the corrugation height. Using the above two definitions, Eq. (3-10) becomes

$$A^{(1)''}(z) \exp\left[-i\rho_z^{(1)}z\right] - 2i\rho_z^{(1)}A^{(1)'}(z) \exp\left(-i\rho_z^{(1)}z\right]$$

$$+ B^{(1)''}(z) \exp\left[i\rho_z^{(1)}z\right] + 2i\rho_z^{(1)}B^{(1)'}(z) \exp\left[i\rho_z^{(1)}z\right]$$

$$- i\left(\frac{2\pi}{\lambda}\right)^2 n_g \frac{n_c^2 - n_g^2}{2n_g} e(\lambda)h(z)A^{(1)}(z) \exp\left[i(2\pi f(z) - \rho_z^{(1)})z\right]$$

$$+i\left(\frac{2\pi}{\lambda}\right)^2 n_g \frac{n_c^2 - n_g^2}{2n_g} e(\lambda)h(z)A^{(1)}(z) \exp\left[-i(2\pi f(z) + \rho_z^{(1)})z\right]$$

$$- i\left(\frac{2\pi}{\lambda}\right)^2 n_g \frac{n_c^2 - n_g^2}{2n_g} e(\lambda)h(z)B^{(1)}(z) \exp\left[i(2\pi f(z) + \rho_z^{(1)}z\right]$$

$$+ i\left(\frac{2\pi}{\lambda}\right)^2 n_g \frac{n_c^2 - n_g^2}{2n_g} e(\lambda)h(z)B^{(1)}(z) \exp\left[-i(2\pi f(z) - \rho_z^{(1)})z\right] = 0 \tag{3-13}$$

Now Eq. (3-13) is identical to Eq. (1-8) if the following quantities are equated.

$$A(z) \leftrightarrow A^{(1)}(z) \tag{3-14a}$$

$$B(z) \leftrightarrow B^{(1)}(z) \tag{3-14b}$$

$$n_0 \leftrightarrow n_g \tag{3-14c}$$

$$\theta_0 \leftrightarrow \theta_g^{(1)}(\lambda) \tag{3-14d}$$

$$\rho_z \leftrightarrow \rho_z^{(1)}(\lambda) \tag{3-14e}$$

$$\Delta n(z) \leftrightarrow \frac{n_c^2 - n_g^2}{2n_g} e(\lambda)h(z) \tag{3-14f}$$

Recall that for any given λ, $\theta_g^{(1)}(\lambda)$, $e(\lambda)$ and $\rho_z^{(1)}(\lambda)$ are known. Thus, if $h(z)$ is also known, Abelès' multilayer dielectric theory, as presented in Chapter 1, can be used to find r. Let us divide the CWF into N sections along the z axis with the reflection and transmission coefficients of the j^{th} section being denoted by r_j and t_j, respectively. Then, as in Section 3,

$$\frac{r}{t} \prod_{j=1}^{N} t_j \simeq op(1) \tag{3-15}$$

and

$$op(1) \simeq \int_{-\infty}^{\infty} \frac{n_c^2 - n_g^2}{2n_g^2 \cos^2 \theta_g^{(1)}(\lambda)} e(\lambda)h'(z) \exp\left[i2Kn_g(\cos \theta_g^{(1)}(\lambda))z\right] dz \tag{3-16}$$

Combining Eqs. (3-15) and (3-16) yields

$$h'(z) = \int_{-\infty}^{\infty} \frac{r}{t}\left(\prod_{j=1}^{N} t_j\right) \frac{2n_g^2 \cos^2 \theta_g^{(1)}(\lambda)}{\left(n_c^2 - n_g^2\right) e(\lambda)} \exp\left[i2Kn_g(\cos \theta_g^{(1)}(\lambda))z\right] d\left(\frac{2n_g \cos \theta_g^{(1)}(\lambda)}{\lambda}\right) \tag{3-17}$$

Using the properties of Fourier transforms Eq. (3-17) becomes

$$h(z) = 2\mathrm{Re}\int_{0}^{\infty} \frac{r}{t}\left(\prod_{j=1}^{N} t_j\right) \frac{2in_g \cos \theta_g^{(1)}(\lambda)}{\left(n_c^2 - n_g^2\right) e(\lambda)} \exp\left[i2Kn_g\left(\cos \theta_g^{(1)}(\lambda)\right)z\right] d\left(\frac{2n_g \cos \theta_g^{(1)}(\lambda)}{\lambda}\right)$$

Thus, if r and t are known as a function of λ, then the iterative technique outlined in Section 3 can be used to determine $h(z)$.

REFERENCES/SECTION 3

1. A. Yariv, Introduction to Optical Electronics (2nd Edition), Chapter 13, Holt, Rinehart and Winston, New York, 1971.